This article has been accepted for publication in a future issue of this journal, but has not been fully edited. Content may change prior to final publication. Citation information: DOI 10.1109/ACCESS.2021.3078570, IEEE Access

IEEE Access
Multidisciplinary ⋮ Rapid Review ⋮ Open Access Journal

Date of publication xxxx 00, 0000, date of current version xxxx 00, 0000.

*Digital Object Identifier 10.1109/ACCESS.2017.Doi Number*

# Damping of Low-Frequency Oscillations in Power Systems by Large-Scale PV Farms: A Comprehensive Review of Control Methods

**Mahdi Saadatmand[1], Gevork B. Gharehpetian[2], (Senior Member, IEEE), Ali Moghassemi[3], Josep M. Guerrero[4], (Fellow, IEEE), Pierluigi Siano[5], (Senior Member, IEEE), Hassan Haes Alhelou[6,7], (Senior Member, IEEE)**
[1] Department of Electrical Engineering, Science and Research Branch, Islamic Azad University, Tehran, Iran
[2] Department of Electrical Engineering, Amirkabir University of Technology, Tehran, Iran
[3] Department of Energy Technology, Aalborg University, 6700 Esbjerg, Denmark
[4] Center for Research on Microgrids (CROM), Department of Energy Technology, Aalborg University, 9220 Aalborg East, Denmark
[5] Department of Management & Innovation Systems, University of Salerno, 84084 Fisciano, Italy
[6] Department of Electrical Power Engineering, Tishreen University, Lattakia 2230, Syria
[7] School of Electrical and Electronic Engineering, University College Dublin, Dublin 4, Ireland

Corresponding author: H. H. Alhelou (e-mail: alhelou@ieee.org).

**ABSTRACT** Global warming and the desire to increase the use of clean energy have led to increasing the installation and operation of renewable energy power plants (REPPs), especially large-scale photovoltaic (PV) farms (LPFs). Given that the LPFs are added to power system or replace conventional power plants, they must be able to perform the basic tasks of synchronous generators (SGs). One of these tasks is the ability to mitigate the low-frequency oscillation (LFO) risk. Also, one of the LPFs problems is reducing the power system inertia and increasing the risk of LFOs. Therefore, these types of power plants must damp the LFOs through a power oscillation damping controller (PODC), similar to the performance of power system stabilizers (PSSs) in the SGs. This paper represents an overview of the different PODCs and control methods for LFOs damping by LPF. It seems that it can be a driver for future studies. Different studies show that the application of PODCs for LPFs can play an effective role to damp the LFOs and increase the power system stability.

**INDEX TERMS** Low-Frequency Oscillation (LFO); First Generation Generic Model (FGGM); Large-scale PV Farm (LPF); Power Oscillation Damping Controller (PODC); Second Generation Generic Model (SGGM); Small-signal stability (SSS)

## NOMENCLATURE

| | |
|---|---|
| AVR | Automatic voltage regulator |
| BESS | Battery energy storage system |
| DAE | Differential-algebraic equations |
| DFIG | Doubly-fed induction generator |
| EPRI | Electric Power Research Institute |
| FACTS | Flexible AC transmission systems |
| FGGM | First generation generic model |
| FFR | Fast frequency response |
| FOPID | Fractional-order PID |
| GE | General Electric |
| GrHDP | Goal representation heuristic dynamic programming |
| HVDC | High voltage direct current |
| HVRCM | High voltage reactive current management |
| ITAE | Integral of time-weighted absolute error |
| IBPP | Inverter-based power plant |
| LLC | Lead-lag compensator |
| LPF | Large-scale PV farm |
| LQG | Linear–quadratic–Gaussian |
| LQR | Linear-quadratic regulator |
| LSSM | Linearized small-signal model |
| LTI | Linear time-invariant |
| LTV | Linear time-varying |
| LFO | Low-frequency oscillation |
| LVACM | Low voltage active current management |
| MMAC | Multiple model adaptive control |
| NERC | North American Electric Reliability Corporation |
| PCC | Point of common coupling |

| | |
|---|---|
| PSO | Particle swarm optimization |
| PSS | Power system stabilizer |
| PID | Proportional-integral-derivative |
| PV | Photovoltaic |
| PV1E | Electrical control model |
| PV1G | PV generator/ converter model |
| PODC | Power oscillation damping controller |
| REPP | Renewable energy power plant |
| REEC_B | Renewable energy electrical control_version B |
| REGC_A | Renewable energy generator/convertor_version A |
| REPC_A | Renewable energy plant controller_version A |
| SG | Synchronous generator |
| SGGM | Second generation generic model |
| SSS | Small-signal stability |
| STATCOM | Static synchronous compensator |
| VSG | Virtual synchronous generator |
| WAMS | Wide-area measurement system |
| WECC | Western Electricity Coordinating Council |

## I. INTRODUCTION

Due to the challenge of global warming and increasing air pollution in the world, in recent years, much attention has been paid to the use of renewable energy resources. One of the most important resources is solar energy [1]. Studies have revealed that the earth's surface receives approximately $1.8\times10^{11}$ MW of power from solar radiation at each instant. This is much more than the total power consumption in the world [2]. Also, studies have shown that the electrical power demand of Europe, the North African region, and the Mediterranean can be supplied by building solar facilities in the Sahara Desert [3]. Figure 1 indicates the world solar energy potential map. As shown in the figure, most of the countries have a high potential for solar power generation [4]. Accordingly, there is a strong desire to install large-scale photovoltaic (PV) farms (LPFs) (>100 MW), and their penetration level is increasing every day [5]. It is estimated that by 2030, the power generation capacity of LPFs worldwide will be more than 3000 TWh [6].

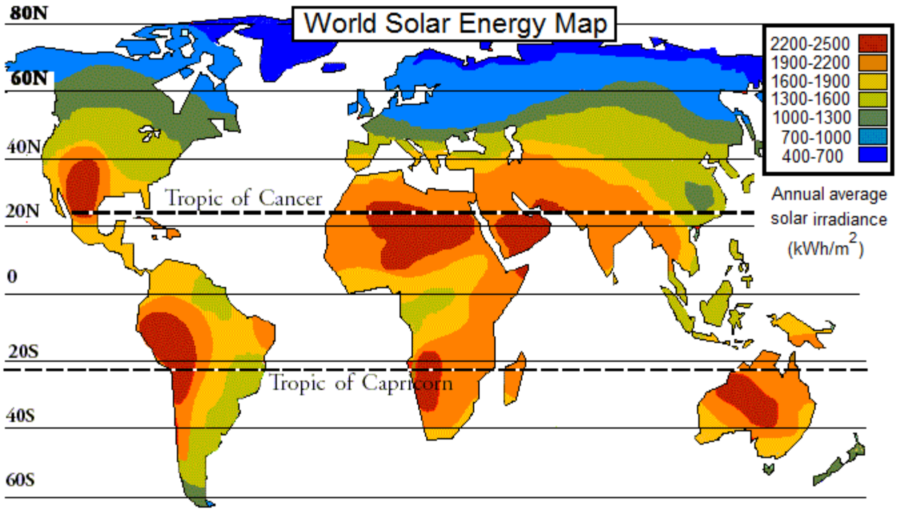

**FIGURE 1.** World solar energy potential map.

LPFs have a different structure from conventional power plants. These types of power plants are based on the inverter and they are classified as inverter-based power plants (IBPPs) [7, 8]. LPF does not have rotating mechanical components. Therefore, they do not have inherent inertia and can reduce the power system inertia [8]. Table I shows a comparison between LPF and conventional power plants. Given the different behavior of these types of power plants than conventional power plants, many studies have been conducted on the effects of LPFs on power system stability [9-18]. The results of studies show that LPFs can strongly increase the risk of low-frequency oscillations (LFOs) and power system instability, by reducing the power system inertia.

TABLE I
COMPARISON BETWEEN LPFS AND CONVENTIONAL POWER PLANTS

| Characteristics | Conventional power plants | LPF |
|---|---|---|
| **Generation uncertainty** | Very low | High |
| **Inertia** | High | No |
| **Maintenance cost** | Moderate | Very low |
| **Capacity factor** | High | Very low |
| **Annual growth in power systems** | High | Very high |

Some mechanisms indicating the indirect effect of the LPF on LFOs are as follows [8]:

- Replacing LPF instead of synchronous generator (SG).

- Impact on synchronization forces due to the effect of LPF on the main transmission lines.
- Interaction between the LPF controls and damping torques of large SGs.

So, with increasing the penetration level of LPFs, two basic issues are raised:

- Considering that LPFs reduce the system inertia, so it is necessary to create inertia through an additional mechanism.
- Due to the increasing penetration level of LPFs, they must be able to do the basic tasks of SGs such as LFOs mitigation by a power oscillation damping controller (PODC).

Based on these two issues, different studies have been done to introduce the control mechanisms to mitigate and damp the LFOs by LPFs based on PODCs design [19-28]. The primary aim of this paper is to investigate the LFOs damping by LPFs in power systems and introduce the control mechanisms. To motivate the research on this important research area, a complete overview on the power system stability is introduced focusing on the rotor angle stability in which the stability of LFOs is one of the important topics. The mathematical representation of small-signal stability (SSS) is then presented. This paper also introduces the LPF models that can be used for LPF modeling in power systems dynamic studies. Furthermore, the structures of used PODCs in LPF to damp LFO are surveyed and discussed. Moreover, this paper highlights the main challenges and research gaps to motivate research on this area to improve the stability of the power systems with the high penetration level of LPFs. Also, problems and challenges related to the design and industrialization of the controllers have been investigated. The opportunities to improve the stability of the power system based on control methods implemented based on wide-area monitoring systems are also highlighted.

The rest of this paper is organized as follows. In Section 2, a brief overview of the power system stability concept and the mathematical basis of SSS are presented. The LPF dynamic models for stability analysis are presented in Section 3. Then, in Section 4 the basis of the LPF damping controller performance is presented. Designed LPF damping controllers are introduced and discussed in Section 5. Also, comparisons and discussions of the types of PODCs are provided in Section 6. The research gaps and opportunities are stated in Section 7. Moreover, the challenges and research gaps are presented in Section 8. Finally, the conclusions are given in Section 9.

## II. POWER SYSTEM STABILITY

The capability of the power system to keep the balance during normal conditions and to restore equilibrium after disturbances is considered as power system stability [29-33]. Power system stability is categorized based on the system response to a disturbance as shown in Figure 2.

This classification can be expressed as follows:

- Rotor angle stability is the ability of the SGs to keep or restore the balance between electromagnetic torque and mechanical torque.
- Frequency stability is defined as the power system's capability to recover the equilibrium between system generation and load demand.
- Voltage stability refers to the power system's capability to keep the steady-state of all bus voltages under normal conditions and after disturbances.

It should be noted that these expressions are the classic classification of power system stability [30, 33]. Recently, in [34, 35], the classic classification has been expanded, and the following two new classes have been added to the classification of power systems stability:

- Converter- driven stability
- Resonance stability

Converter- driven stability involves dynamic interactions between control systems of power electronic-based systems and the power system devices [34, 35]. Also, the impact of high voltage direct current (HVDC) and flexible AC transmission systems (FACTS) on torsional and effect of doubly-fed induction generator (DFIG) controls on electrical resonance stability are expressed in the resonance stability [34, 35].

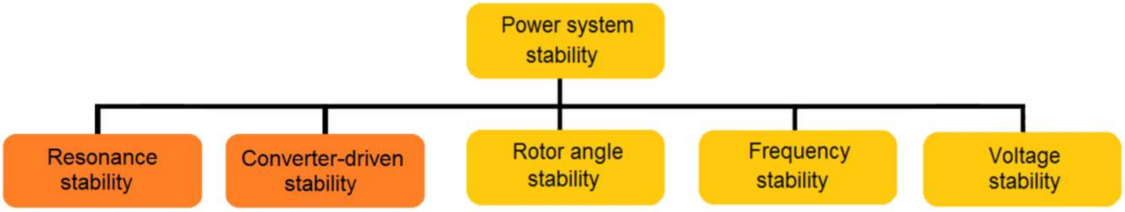

**FIGURE 2.** **Power system stability classification.**

As shown in Figure 3, rotor angle stability is categorized into two various categories: transient stability and SSS [36-40]. Transient stability is the power system's ability to keep the synchronism when it's exposed to a severe disturbance [29, 30]. The impact of small disturbances on the power system variables such as low variations in load and power generation [32, 36] is defined in SSS studies [36, 37]. The SSS is classified into two different classes. Oscillatory state due to lack of damping torque and non-oscillatory state due to lack of synchronizing torque [36, 37]. The damping torque is the component of torque that is in phase with the speed deviation. Also, the synchronizing torque is the component of the torque that is in phase with the rotor angle deviation.

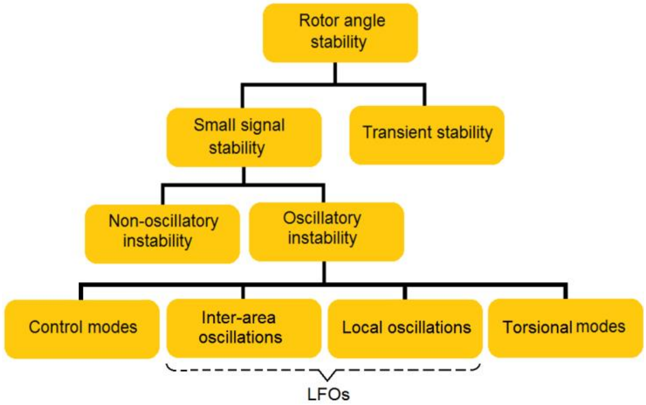

**FIGURE 3.** **Classification of the rotor angle stability.**

The problem of non-oscillatory states has been largely solved using an Automatic Voltage Regulator (AVR) in the excitation system of SG [36, 37]. Also, oscillatory states are usually damped using PSS. In oscillatory states, oscillation with a frequency between 0.1 Hz to 2 Hz is called LFO [36]. This oscillation can be divided into two general categories as follows [36]:

- Inter-area oscillation with a frequency range of 0.1-1.0 Hz.
- Local oscillation with a frequency range of 1.0-2.0 Hz.

Inter-area oscillation is caused by the oscillation of a group of generators or power plants in an area relative to generators or power plants in another area, while local oscillation is caused by the oscillation of a generator or a power plant relative to a generator or power plant in the same area [36].

### A. CONCEPT OF SSS AND MATHEMATICAL BACKGROUND

Power systems are non-linear dynamic systems that are considered by a set of non-linear differential-algebraic equations (DAE) [41, 42]. To power system analysis these equations usually explained using state-space equations as follows [28, 29]:

$$\dot{x} = f(x,u) = Ax + Bu \quad (1)$$

$$y = g(x,u) = Cx + Du \quad (2)$$

where $x = [x_1, \dots, x_n]^T$ is the vector of the state variables, $y = [y_1, \dots, y_n]^T$is the vector of the system output, $u = [u_1, \dots, u_n]^T$is the vector of the system input, $A$ is the state matrix, $B$ is the input matrix, $C$ is the output matrix and, $D$ is a matrix describing the direct connection between input and output matrices. Also, $f$ and $g$ are the vectors of non-linear functions.

A popular method for SSS analysis is the modal analysis or eigenvalues analysis. To use this method, it is necessary to linearize the power system. Therefore, the power system described by (1) and (2) is linearized around an operating point [29, 30]. So, the power system can be stated as a linear system:

$$\Delta\dot{x} = A\Delta x + B\Delta u \quad (3)$$

$$\Delta y = C\Delta x + D\Delta u \quad (4)$$

where $\Delta$ remarks a small variation around the operating point. Based on modal analysis, the power system stability can be investigated by calculating the eigenvalues of state matrix. It should be noted that, the eigenvalues are the roots of the system characteristic equation $det(sI - A) = 0$, where $det$ is the determinant. Each eigenvalue can be expressed as follows:

$$\lambda_i = \sigma_i \pm j\omega_i \quad (5)$$

Based on the first method of Lyapunov [43, 44], the linear system in (3) and (4) is stable if and only if:

$$|arg\ (eig(A))| > \pi/2 \quad (6)$$

where $eig(A)$ indicates the eigenvalue of the system matrix. Therefore, by evaluating the eigenvalues, the power system stability can be determined. It should be noted that in some cases due to the use of some non-linear elements and devices in controllers such as limiters and dead-bands, the power system model is strongly non-linear and the values related to the linear approximation do not give the correct results. In this case, the use of modal analysis is impossible and the non-linear time-domain analysis is used.

## III. LPF MODELS FOR STABILITY ANALYSIS

The LPF includes three basic parts, the PV array, inverter, and the controller as shown in Figure 4. For power system stability analysis, it is necessary to, the steady-state and dynamic models of LPF are available [5, 45-47]. So, it should describe the LPF models for steady-state and dynamic analysis.

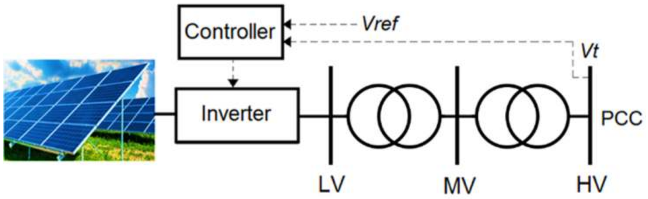

**FIGURE 4.** **Schematic structure of the LPF.**

### A. LPF MODEL FOR STEADY-STATE STUDIES

To study the power system's behavior in steady-state, the steady-state models of all system devices must be defined. Given that renewable energy power plants (REPPs) are the important components of modern power systems, so, having a steady-state model of this type of power plant is essential. Accordingly, the LPF is modeled into a single generator model for steady-state analysis. This model is called simple aggregate model [5, 47-51]. The simple

This article has been accepted for publication in a future issue of this journal, but has not been fully edited. Content may change prior to final publication. Citation information: DOI 10.1109/ACCESS.2021.3078570, IEEE Access

aggregated model is shown in Figure 5. This model has a power rating equal to the LPF power rating and connected to the point of common coupling (PCC). Since these types of power plants have reactive power generation/ absorption ability, the LPF, like SG, is considered for steady-state analysis, i.e. its bus is a PQ or PV bus [49,50].

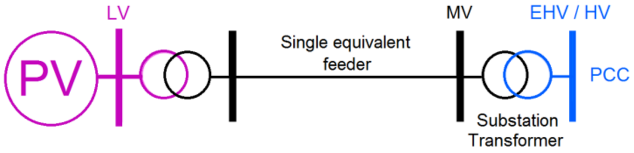

**FIGURE 5.** **The simple aggregated model for PF.**

### *B. LPF MODELS FOR DYNAMIC STUDIES*

From the beginning of the 21st century, with the increasing desire to install and operate LPFs, operators and owners of LPFs needed to model the LPF to evaluate its performance in different operating conditions [52-55]. Until then, a generic and standard model was not available; therefore, they used the user-written model files in many software tools such as GE PSLF and Siemens PSSE [56]. For the first in 2010, General Electric (GE) introduced a generic standard model called the First Generation Generic Model (FGGM) [49]. Also, in a study in 2011 [57], the FGGM was examined. In 2012, Western Electricity Coordinating Council (WECC) published a guide for the LPF dynamic model [58]. This guide is considered to serve for the LPF's model to be implemented for power system analysis and simulations. Later this model was named the Second Generation Generic Model (SGGM). The SGGM is currently being developed in collaboration with WECC and Electric Power Research Institute (EPRI) [48, 50]. It should be noted that this model can only be used for the positive sequence in the steady-state analysis [48, 59]. In the continuation of this section, these two models are investigated.

#### 1) FGGM FOR LPF MODELING

This subsection discusses the structure and functionalities of FGGM. This model has two components as shown in Figure 6 [49, 57].

- PV GENERATOR/ CONVERTER MODEL (PV1G)

This model is equivalent to the LPF converters and plays the interface role between the LPF and the power system [49, 56]. Since this was the first generation of the LPF model, so the number 1 shows its generation. The PV1G schematic is shown in Figure 7. When running this model, the MVA rating of the LPF is equal to the total MVA rating of the PVGs inside the PF. PV1G model is a simple display of inverter protection and time-delay of the inverter controlling system. The 0.02-seconds time-delay provides a proper approximation of control system delay [56].

The inverter of LPF is the current controlled device and its performance is very dependent on current thermal limits [56]. For this purpose, the high voltage reactive current management (HVRCM) module is used to detect the injected reactive current [48, 49]. If the terminal voltage of the inverter is increased from the set $V_{olim}$ value, the HVRCM module limits the increase in the reactive current injection by decreasing the terminal voltage. Also, the low voltage active current management (LVACM) module limits the increase in the active current during the low voltage events, based on the current limitations [59-63].

In other words, the HVRCM and LVACM modules are considered for the thermal protection modeling of the power switches (IGBT and diode). This type of protection is based on the current-carrying capability of the power switches [62].

- ELECTRICAL CONTROL MODEL (PV1E)

The PV1E model sends the active and reactive currents command to the PV1G model. The schematic of this controller is depicted in Figure 8 [49, 57].

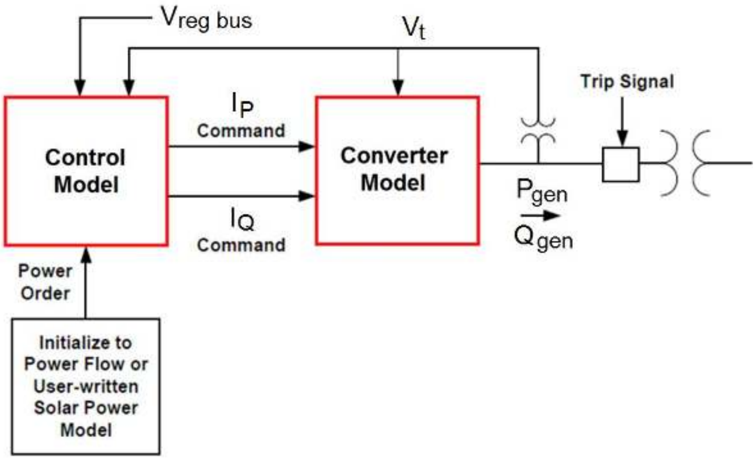

**FIGURE 6.** **Overall structure of FGGM.**

This article has been accepted for publication in a future issue of this journal, but has not been fully edited. Content may change prior to final publication. Citation information: DOI 10.1109/ACCESS.2021.3078570, IEEE Access

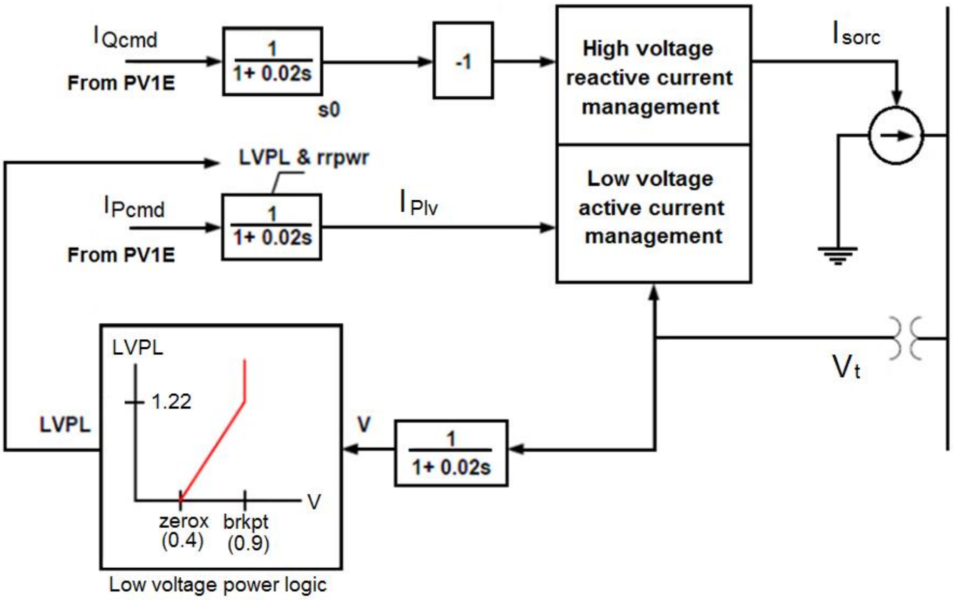

**FIGURE 7.** **PV1G model block diagram.**

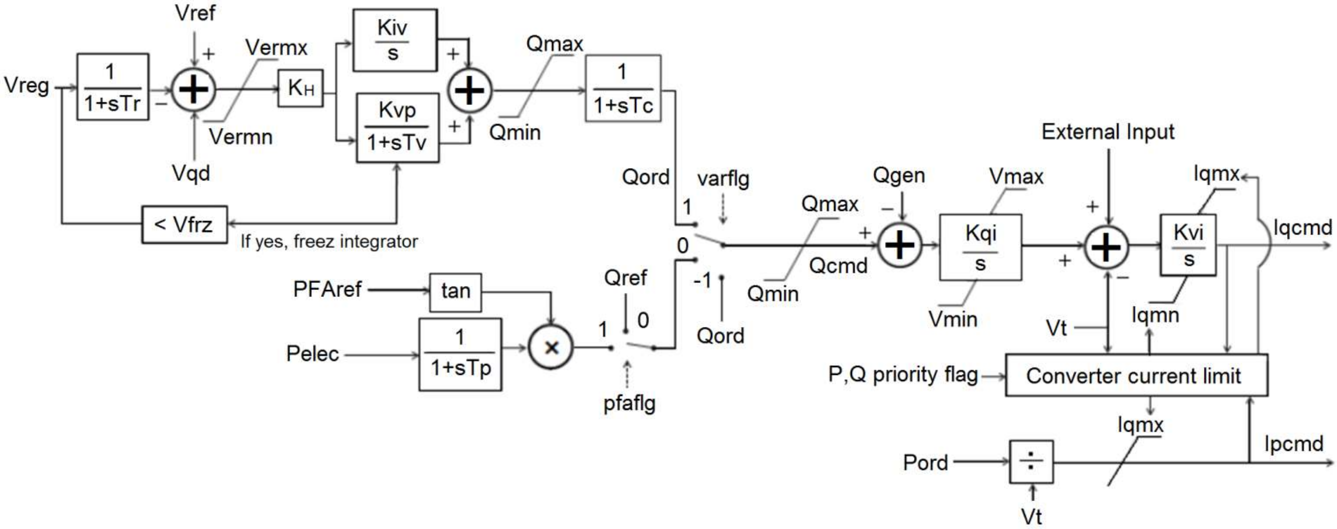

**FIGURE 8.** **PV1E model block diagram.**

### 2) SGGM FOR LPF MODELING

This model is actually an upgrade of the FGGM that has a central control module. The SGGM is WECC approved [48, 51, 61]. The schematic structure of SGGM is depicted in Figure 9 [48]. This model includes three modules, inverter protection module named renewable energy generator/convertor_version A (REGC_A), an electrical controller module for local power control named renewable energy electrical control_version B (REEC_B), and a central control module for power control at plant-level named renewable energy plant controller_version A (REPC_A) [48, 61].

- REGC_A MODULE

The REGC_A is similar to the PV1G model [48, 61]. It combines a high bandwidth current regulator that injects the command signals ($I_q$, $I_p$) into the inverter model in response to command signals ($I_{qcmd}$, $I_{pcmd}$) from REEC_ B. This module is depicted in Figure 10 [48, 61].

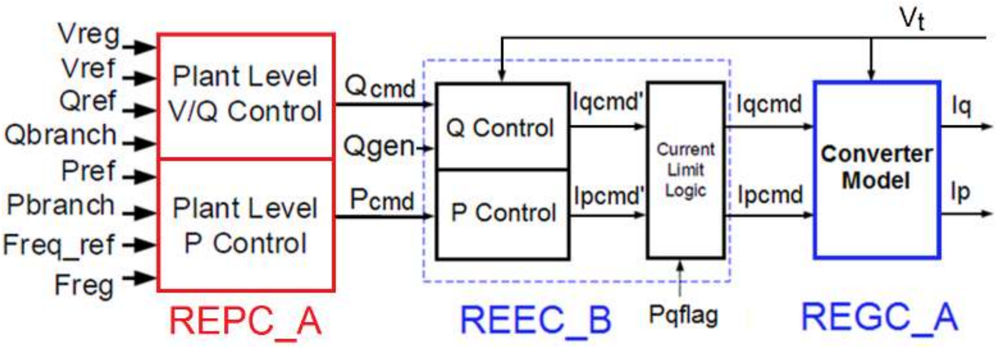

FIGURE 9. Overall structure of SGGM.

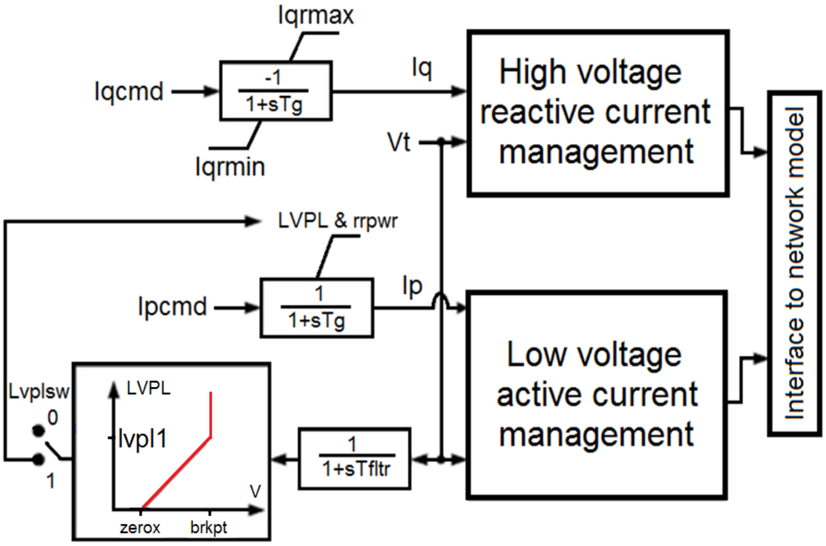

FIGURE 10. Schematic structure of REGC_A model.

- REEC_B MODULE

The REEC_B module includes two separate control loops. A local active power control loop and a local reactive power control loop [48, 61].

**A- Local active power control:** This is a control loop that provides the active current command as a command signal to the REGC_A module. Note that the command signal is subject to the thermal limitations of the power electronic switches, as well as the priority between active and reactive currents [48, 61].

**B- Local reactive power control:** This is a control loop that provides the reactive current command to the REGC_A model. The command signal is subject to current limiting. The following control states are considered [48, 61]:

- Constant power factor state, based on the inverter power factor in steady-state.
- Constant reactive power state, based either on the inverter absolute reactive power in the steady-state or reactive power from the central controller.

As shown in Figure 11, there are several flags in this module that are used to determine different control strategies in the local control mode [48, 61].

- REPC_A MODULE

The REPC_A model demonstrates the central controller model behavior [48, 51, 61]. This model is optional because not all LPFs are constructed with the central controller. The REPC_A model provides the plant-level control commands to the REEC_B. The schematic of this model is depicted in Figure 12 [48, 51, 61]. This model transmits the command signals to the inverters controllers.

This model includes the features as below:

- Regulation of remote bus voltage through the voltage control loop. This is done by compensating for the line drop.
- Regulation of the reactive power of the selected branch.
- Provides governor response at plant-level based on the frequency deviation of a remote bus.

This article has been accepted for publication in a future issue of this journal, but has not been fully edited. Content may change prior to final publication. Citation information: DOI 10.1109/ACCESS.2021.3078570, IEEE Access

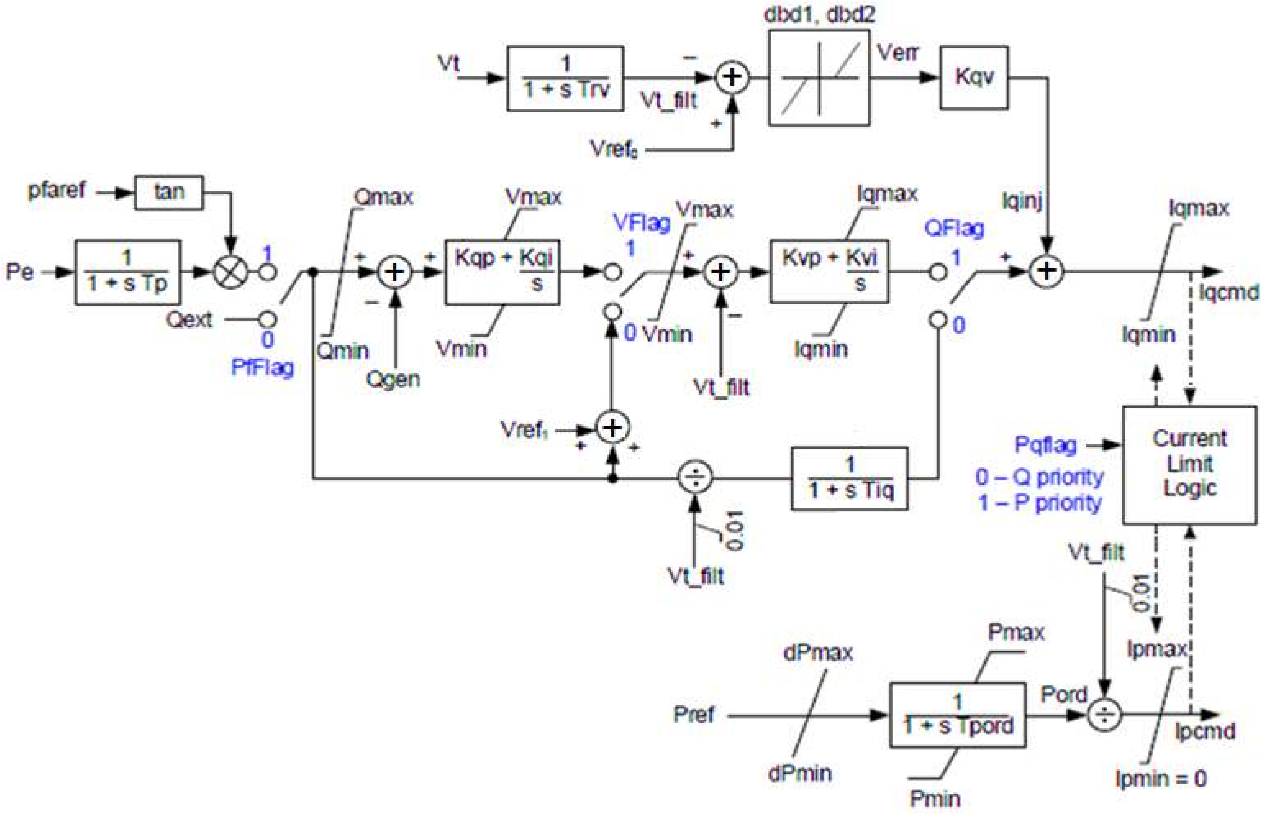

**FIGURE 11.** Schematic structure of REEC_B model.

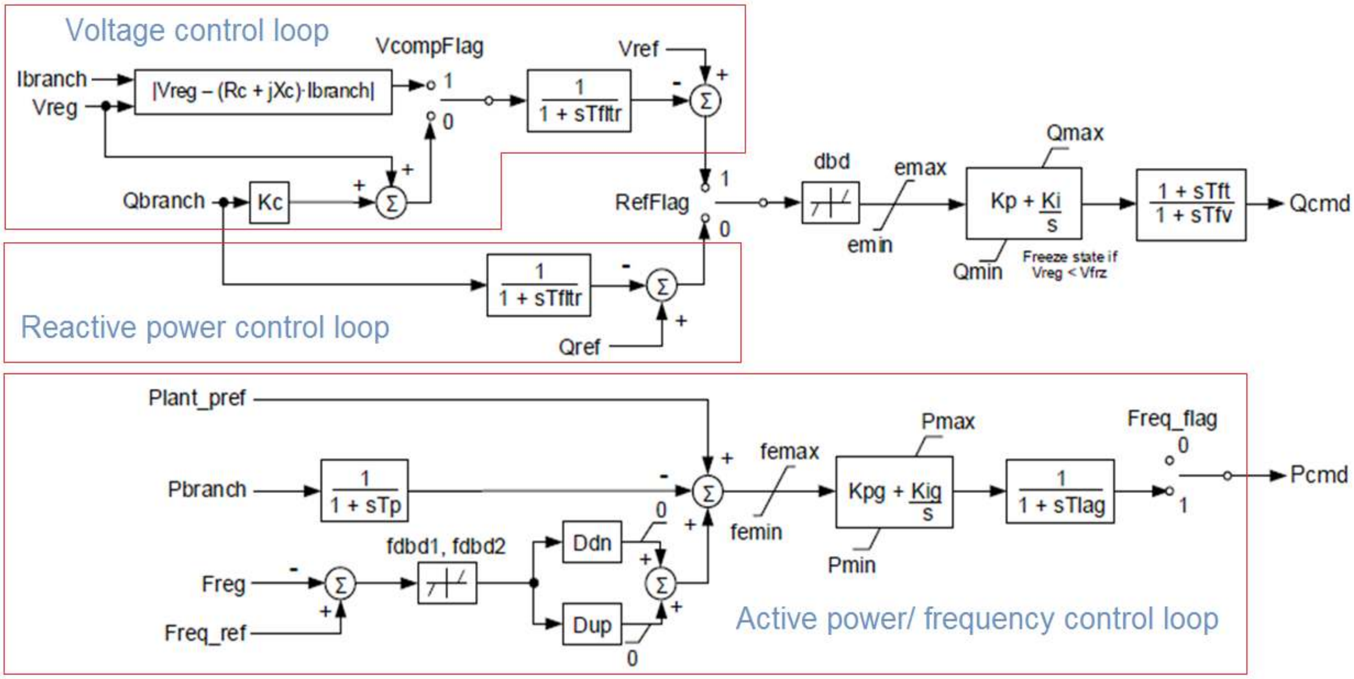

**FIGURE 12.** Schematic structure of REPC_A model.

This article has been accepted for publication in a future issue of this journal, but has not been fully edited. Content may change prior to final publication. Citation information: DOI 10.1109/ACCESS.2021.3078570, IEEE Access

It should be noted that, with different flags in the SGGM, the PF can have many control strategies for various operating conditions. The flag setting and input parameter settings for the different strategies to control the active and reactive power are described in [48, 61].

Due to the non-linearity of these models, they have extensive and complex relationships. A more complete explanation of these models is available in [62] and [63]. Typical values of the parameters of these models and internal variables are listed in the appendix [61].

A general comparison of the capabilities of these models is listed in Table II.

TABLE II
GENERAL COMPARISON BETWEEN FGGM AND SGGM

| **Specification/Capabilities** | **Dynamic model** | |
|---|---|---|
| | **FGGM** | **SGGM** |
| **Electrical controls** | ✓ | ✓ |
| **Grid interface** | ✓ | ✓ |
| **Voltage/ frequency protection** | ✓ | ✓ |
| **Governor response** | - | ✓ |
| **Plant controller (Central)** | - | ✓ |
| **Voltage regulation at a remote bus** | - | ✓ |
| **Reactive power regulation on a remote line** | - | ✓ |
| **Usable for hybrid power plants** | - | ✓ |

## IV. THE BASIS OF THE LPF DAMPING CONTROLLER PERFORMANCE

The LFO of the power system occurs mainly due to the lack of equilibrium between electrical torque and mechanical torque [29-33]. In this section, to show the effect of the LPF based PODC for LFO damping, inter-area oscillation is considered as LFO in a simple two-area system [64, 65]. For this purpose, any area has been considered as an equivalent SG. As shown in Figure 13 both areas are connected through a transmission line. Also, each area contains a local load. In this system, LPF is integrated with area 1.

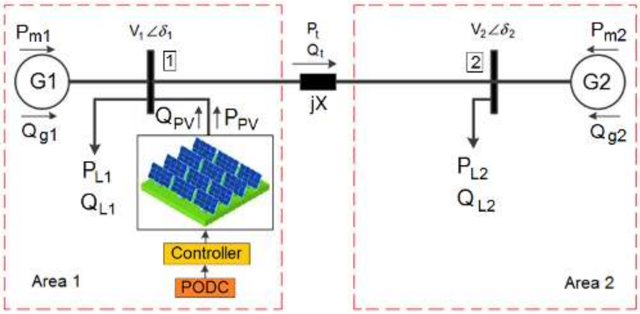

FIGURE 13. Simple structure of a two-area test system.

The dynamic performance without LPF can be explained using the swing equation as follows [64, 65]:

$$\frac{d\delta_{12}}{dt} = \omega_{12} \tag{7}$$

$$\begin{aligned}\frac{d\omega_{12}}{dt} &= \frac{1}{H_1}(P_{m1} - P_{L1}) - \frac{1}{H_2}(P_{m2} - P_{L2}) \\ &\quad - \left(\frac{1}{H_1} + \frac{1}{H_2}\right)\left(\frac{V_1 V_2}{X}\right) sin\, \delta_{12}\end{aligned} \tag{8}$$

where $\delta_{12} = (\delta_1 - \delta_2)$ and $\omega_{12} = (\omega_1 - \omega_2)$ represent the generators rotor angle difference between the two areas and generators speed difference between the two areas, respectively. When the LPF is connected to area 1, (8) can be considered as follows:

$$\begin{aligned}\frac{d\omega_{12}}{dt} &= \frac{1}{H_1}(P_{m1} + P_{PV} - P_{L1}) - \frac{1}{H_2}(P_{m2} - P_{L2}) \\ &\quad - \left(\frac{1}{H_1} + \frac{1}{H_2}\right)\left(\frac{V_1 V_2}{X}\right) sin\, \delta_{12}\end{aligned} \tag{9}$$

As shown in the third part of (9), the transmitted active power from area 1 to area 2 is related to the angle difference between the two areas. Also, the transmitted reactive power is related to the voltage magnitude, as follows [65-67]:

$$Q_t = Q_{g1} - Q_{L1} + Q_{PV} = \frac{V_2^2 - V_1 V_2 \cos \delta_{12}}{X} \tag{10}$$

where $Q_t$ is the transmitted reactive power from area 1 to area 2, $Q_{PV}$ is the reactive power injected from LPF to the grid, and $Q_{L1}$ is the reactive power consumption by loads of area 1. In the steady-state condition, the SGs operate synchronously in the two areas. In this condition the generators rotor angle difference between the two areas $\delta_{12}$ is constant, and the generators speed difference between the two areas $\omega_{12}$ is equal to zero. However, when a disturbance occurs, the equilibrium between electrical power and mechanical power of generators is lost, which may lead to the inter-area oscillation between the two areas. Therefore, to maintain the SSS, it is necessary to damp the LFOs quickly. As shown in (10), the LPFs can compensate for the reactive power. Therefore, these types of power plants can control the bus voltage. Therefore, LFOs can be damped by controlling the bus voltage. It is done by injecting additional reactive power to the grid in disturbances conditions. For this purpose, an auxiliary controller can be used as a PODC, such as the PSS operation in the SG excitation system.

## V. LPF damping controllers

As shown in the previous section, the use of an auxiliary controller can be a good solution for LFO damping by LPFs. Many studies have been done on the effect of LPFs on the power systems stability, but little study has been done on the PODC design and LFO damping by LPFs. It seems that in the future more advanced types of controllers will be introduced as PODC. In the continuation of this section, the introduced controllers are reviewed.

### A. *LEAD-LAG COMPENSATOR* (LLC)

The simplest and most common type of PODC is the LLC. These types of controllers are used as a common structure of current PSSs. The conventional and popular type of these controllers is the 2nd order single-input LLC, which its use is common in the industry due to its simple structure and easy tuning [67-70]. The control block diagram of this type of controller is depicted in Figure 14 [67-69].

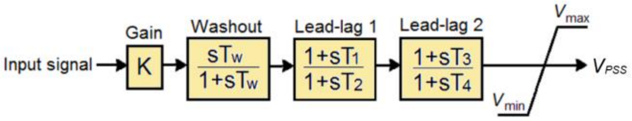

**FIGURE 14.** The 2nd order single-input LLC.

where $K$ is the gain of controller, $T_w$ is the time constant of washout filter, and $T_1$, $T_2$, $T_3$, and $T_4$ are the time constants.

In a study in 2017 [19], an LLC was proposed as PODC for LPF. In the study, an adaptive PODC based on goal representation heuristic dynamic programming (GrHDP) algorithm was proposed. By GrHDP, the adaptive PODC does not require a power system model and is compatible with various operating conditions. Moreover, an adaptive delay compensator is also employed for the proposed PODC to compensate for the communication delay existing in the wide-area measurement system (WAMS). The simulation results showed that the proposed PODC can provide satisfactory damping performance and compensate for the communication delay.

Another study in 2019 [20] proposed a new fast frequency response (FFR) and LFOs damping control by LPFs controlled as static synchronous compensator (STATCOM), termed PV-STATCOM, for simultaneously enhance frequency regulation and SSS of power systems. As shown in Figure 15 the study used the SGGM for LPF modeling. Moreover, an LLC based PODC proposed for LFOs damping in the voltage control loop of REPC_A. Also, a FFR controller has been suggested for frequency control in the active power control loop of REPC_A. Then, the LLC has been tuned using a residue-based method [37]. The simulation results showed the proper performance of the proposed composite control to compensating for the frequency deviation, damping the LFOs, and voltage regulation during disturbances.

The proposed inverter control made effective utilization of the PV inverter capacity and available solar power. Also, it was shown to be superior to the conventional droop control recommended by North American Electric Reliability Corporation (NERC) for generating plants.

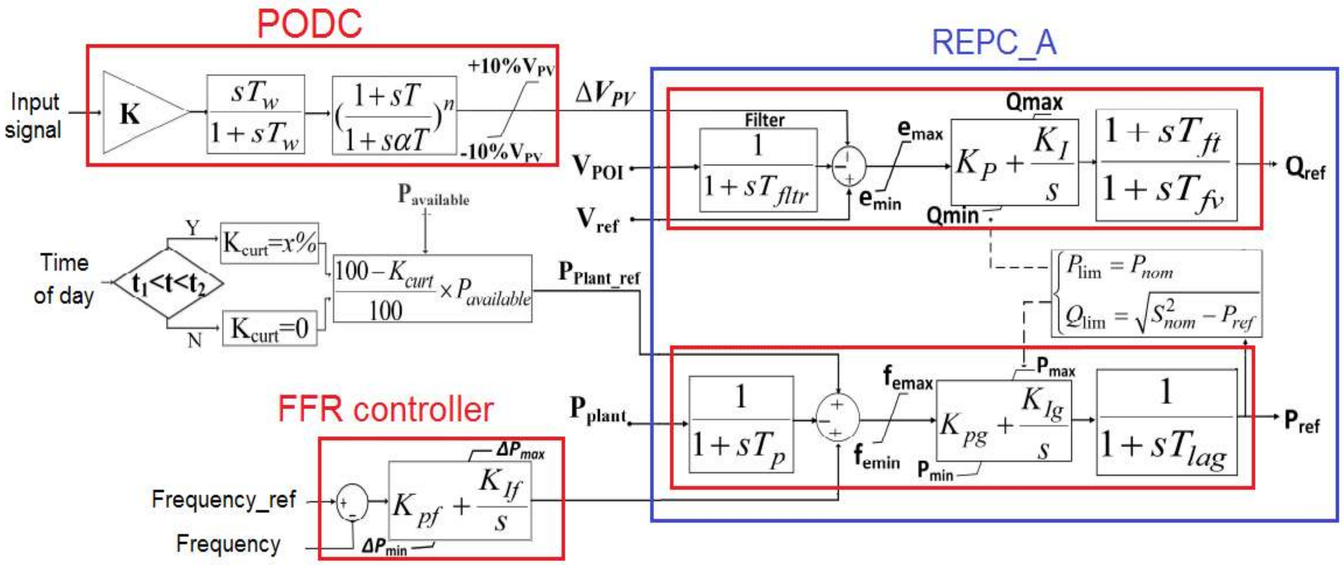

**FIGURE 15.** FFR controller and LLC scheme in REPC_A module.

In another study in 2019 [21], the LFO damping was proposed by an optimal LLC based PODC. The proposed PODC structure was a single-input 2nd order LLC. In the study, the SGGM was used for LPF modeling. Moreover, the PSO algorithm has been used to determine the values of LLC parameters. In fact, PODC was optimally designed. Then the robustness of PODC was assessed in the different operating and loading conditions. The simulation results demonstrated the proper performance of the proposed PODC for the wide range of operating conditions.

The communication delay that occurs inherently in the WAMS negatively affects the SSS. This issue is stochastic in nature and needs to be considered as one of the system uncertainties in smart grids and future systems. Therefore, this issue needs to be considered in PODC design.

Accordingly, in 2019 [22] a probabilistic method has been proposed for PODC tuning under stochastic time delay and under other power system uncertainties arising due to REPPs and loads. In the study, the LLC has been proposed as a PODC in LPF model. Also, the mitigation strategy has been used for the objective function definition. Moreover, the optimization method has been used for PODC design. The results showed that tuning the PODC using the proposed method greatly improves the SSS under various operating conditions. Also, the tuned PODC is robust against time delay uncertainty and other power system uncertainties.

### B. PROPORTIONAL-INTEGRAL-DERIVATIVE (PID) CONTROLLER

Recently, various types of controllers have been introduced in power system applications. Among them the PID controller is known as a simple and efficient controller [71-73]. This type of controller has been widely used in industries because of its simple structure and robust performance in different operating conditions. The simple design and simple structure of the PID controller have led to its widespread use in industries to improve dynamic response and reduce steady-state error [74-78]. Its transfer function is in the form of:

$$Y(t) = K_P\, R(t) + (K_I \int_0^t R(x)dx) + K_D \frac{dR(t)}{dt} \qquad (11)$$

where $K_P$, $K_I$, and $K_D$ represent the proportional, integral, and derivative gains, respectively [71-78]. The PID transfer function in the Laplace domain is as follows:

$$H(S) = \frac{Y(S)}{R(S)} = K_P + \frac{K_I}{S} + +K_D\, S \qquad (12)$$

where $S$ is the complex frequency. The schematic block diagram of this type of controller is shown in Figure 16.

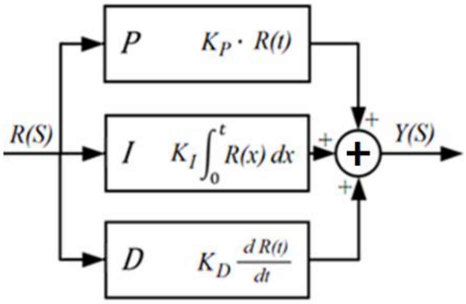

**FIGURE 16.** **PID controller structure.**

Recently in 2020 [23], a general technique to damp the LFOs by LPFs has been proposed. In the study, the optimal PID controller was used as a PODC. For this purpose, the PODC was optimally tuned by the particle swarm optimization (PSO) algorithm [70, 78-81]. Finally, the performance of the proposed PODC was examined in a two-area benchmark system [82]. The results of the study showed the proper performance of the proposed PODC in the wide range of operating conditions. Also, in the study, the results were compared with the performance of LLCs.

### C. LINEAR-QUADRATIC-GAUSSIAN (LQG) CONTROLLER

The performance of the LQG controller is based on the minimization of an objective function that penalizes the state's deviations and actuator's actions during transient terms [83, 84]. The basic idea of the LQG controller design is to address the intrinsic compromise between an attempt to minimize the error and an attempt to maintain control effort at the minimum. This type of controller is the combination of a linear-quadratic regulator (LQR) with a Kalman filter [84]. The LQG controllers can be applied to both linear time-invariant (LTI) systems as well as linear time-varying (LTV) systems [85]. Therefore, it is possible to design the linear feedback controllers for non-linear uncertain systems.

As shown earlier, the general state-space equations explain by (1) and (2). By ignoring the D matrix and considering the process and sensor noise inputs for a plant, these equations can be written as follows [24, 25]:

$$\dot{x} = Ax + Bu + \Gamma w \qquad (13)$$

$$y = Cx + v \qquad (14)$$

where $w$ and $v$ are the process and sensor noise inputs, respectively. To determine the LQG controller parameters it is necessary to obtain an optimal control that minimizes the objective function. The objective function is expressed as bellow [24]:

$$J = \lim_{T\to\infty} \frac{1}{T}\, E\left[\int_0^T (x^T Q x + u^T R u)\, d\tau\right] \qquad (15)$$

where $Q$ and $R$ are weighting matrices such that $Q^T = Q$ and $R^T = R$. By the separation principle, LQG can be divided into two following sub-problems:

- The LQR Problem or determine the optimal state-feedback control. This issue is given by [20, 83-85]:

$$u = -K_C x \qquad (16)$$

$$K_C = R^{-1} B^T P_C \qquad (17)$$

where $P_C$ is a symmetric positive semi-definite solution of the Riccati equation, as follows:

$$A^T P_C + P_C\, A + Q - P_C\, R^{-1}\, B_T\, P_C = 0 \qquad (18)$$

- LQE Problem or the required state's estimation

  Measuring all the states is impossible practically, thus, a Kalman filter is employed to provide the required estimates as an estimator. The Kalman filter structure is that of an ordinary state-estimator with [24]:

$$\dot{\hat{x}} = A\,\hat{x} + Bu + K_f\,(y - C\hat{x}) \qquad (19)$$

$$K_f = P_f\, C^T\, V^{-1} \qquad (20)$$

where $K_f$ is the Kalman filter and $P_f$ is a symmetric positive semi-definite solution of the Riccati equation:

$$P_f\, A^T + A\, P_f + \Gamma w \Gamma^T - P_f\, C^T V^{-1} C\, P_f = 0 \qquad (21)$$

Finally, the optimal control formula of LQG becomes:

$$u = -K_C\, \hat{x} \qquad (22)$$

The structure of the LQG controller is depicted in Figure 17 [83-85].

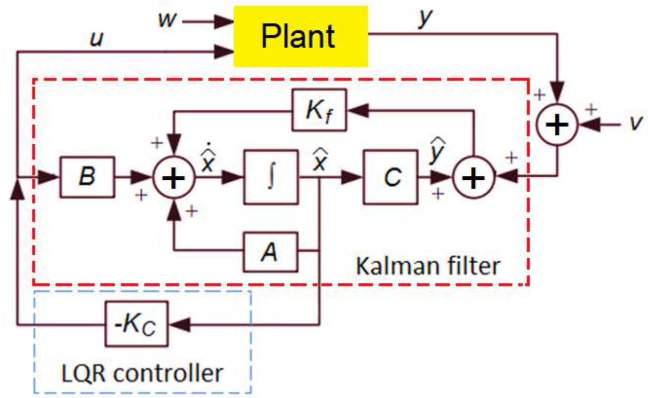

**FIGURE 17.** **LQG controller structure.**

In 2013 [24], a minimax LQG-based controller was proposed for use in LPFs as PODC. For this purpose, the FGGM was used as an LPF dynamic model and, the two-area benchmark system was used for power system simulation. Then the performance of the proposed PODC was evaluated considering feedback signal transmission delay. The simulation results demonstrated that the proposed controller for LPF provides sufficient damping to the LFOs for a wide range of operating conditions and disturbances. This issue also has been investigated in [25].

### *D. MULTIPLE MODEL ADAPTIVE CONTROL (MMAC) STRATEGIES*

For a power system, different scenarios can be considered for post-event conditions. Events include a severe fault in the grid, the sudden outage of a big load, generator, or tie-line, and etc. Then, based on each event, a linearized small-signal model (LSSM) can be considered for the system status after the event.

In a study in 2004 [86], a total of 12 LSSMs have been considered to cover the whole space of anticipated response of the system after an event. Note that, each one of the LSSMs must be located in the model bank.

A general overview of the conventional MMAC strategy is depicted in Figure 18 [86]. The recursive algorithm uses a bank of linearized plant models such as LSSMs in [86], to capture the possible system dynamics following an event [86]. One separate controller is designed, a priori, based on each model from the model bank. At each simulation phase, the actual response is compared with the response of the linearized models which are driven by the same control input [87]. The differences in the response of each model concerning the actual system response are used to generate individual model residuals.

Using these residuals, the probability of each model representing the actual system response is computed. Based on the probabilities, proper weights are assigned to individual control moves such that the less probable models carry less weight [86]. This ensures that the controllers designed for less probable models influence the final control move to a lesser extent [86]. At each level of the recursive algorithm, primarily two tasks are performed, i.e., calculation of probability using a Bayesian approach and assigning suitable weights based on the value of probability [86].

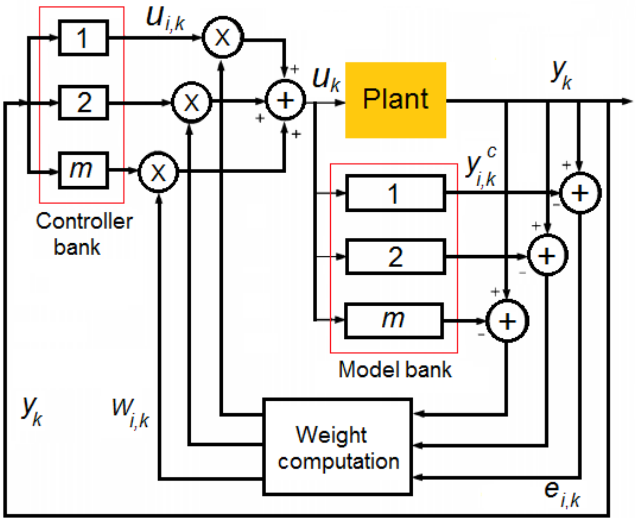

**FIGURE 18.** **Schematic structure of MMAC strategy.**

In 2017 [26], the MMAC has been applied as a control strategy to mitigate the LFOs by LPFs. In the study, the *K*-means clustering algorithm was used taking inter-area modes as features for operating condition clustering and, a common damper was designed for each cluster to reduce the scales of the model bank and the damper bank. Based on the deviation between the output dynamic responses of the actual system and models, the Bayesian approach was employed to calculate the probability of each model representing the actual system in real-time. The non-linear simulation results indicated that the suggested control strategy can damp the LFOs in unexpected operating conditions without any prior knowledge about the post-disturbance state. It should be noted that the FGGM has been used for LPF modeling in the study.

### *E. FRACTIONAL-ORDER PID (FOPID) CONTROLLER*

This type of controller is the general form of a typical PID controller. The mathematical structure of the FOPID controller is based on the fractional-order calculus, which is an effective tool for modeling many phenomena in engineering [88-90]. These types of controllers provide robust performance and wide range of stability area than the conventional PID controllers due to the additional degree of freedom caused by the fractional-orders of integral and derivative [91-95]. Other advantages of this controller include high flexibility in tuning, distortion rejection and high reliability of the model in non-linear applications [88-90]. The FOPID controller is a new approach in electrical engineering for robust controllers tuning with a wide stability area. The standard form of the fractional differential equation of this controller is as below [90-95]:

$$Y(t) = K_P\, R(t) + K_I\, D_t^{-\lambda}\, R(t) + K_D\, D_t^{\delta}\, R(t) \quad (23)$$

Based on (23), the transfer function, $H(s)$, in Laplace-domain is as follows [91, 93]:

$$H(s) = \frac{Y(s)}{R(s)} = K_P + K_I s^{-\lambda} + K_D s^{\delta} \quad (24)$$

where $R(s)$ is the input signal, and $Y(s)$ is the output signal. Moreover, $K_P$, $K_I$ and $K_D$ present the proportional, integral, and derivative gains. In addition, $\lambda$ and $\delta$ show the orders of integral and derivative. The schematic of the FOPID controller in a control loop is shown in Figure 19 [93].

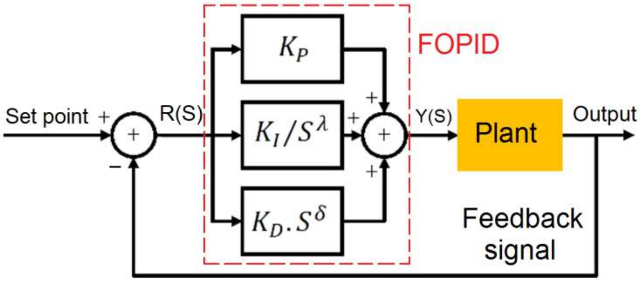

FIGURE 19. **The FOPID controller structure.**

As shown in Figure 20, the orders of integral and derivative of this type of controller, unlike the PID controller, have a wide range. This provides robustness and flexibility to the system and increases the range of power system stability [93-95].

In 2020 [27] the idea of the FOPID controller application in the dynamic model of IBPPs was first proposed. In the study, an LPF was used as a case study in a two-area test system [82]. Also, the SGGM is used for the LPF model. Then the PODC tuning is performed based on the optimization method in the time-domain. In the study, adjustment of FOPID controller parameters was obtained using PSO optimization, and the objective function was defined based on the integral of time-weighted absolute error (ITAE) index [96]. The result of the research indicated the better performance of the proposed PODC than LLC and LQG controller.

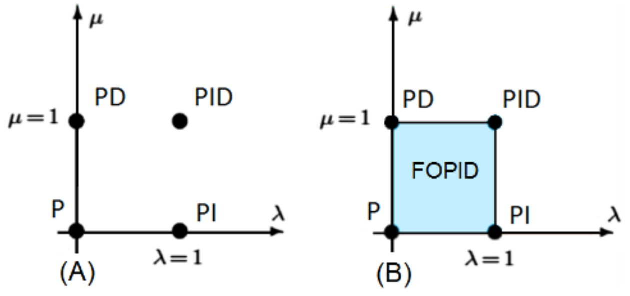

FIGURE 20. **FOPID and PID controllers, from points to plane, (a) integer-order, and (b) fractional-order.**

Recently in 2021 [28], a method was proposed to the coordinated tuning of FOPID-PODC controller with PSS of SGs to damp the LFOs. The study also used SGGM for LPF modeling. In addition, the coordinated tuning was performed based on the PSO algorithm in the time-domain. The results of the research showed the robustness of the proposed PODC against a wide range of events and power system uncertainties.

In both studies, the PODCs are considered in the Q/V control loop of SGGM. As depicted in Figure 21, the study proposed two various points for the PODC in the REPC_B module. Each point can be considered based on the IBPP control strategy.

It should be noted that in the literature, the PODC has been connected to the Q/V control loop, therefore the LPF injects additional reactive power into the power system under disturbance conditions. This is the LFO damping mechanism by LPF, which is described in Section IV.

## VI. SIMULATION RESULS AND COMPARISON

Given that SSS analysis and simulation of LFOs are required, a standard power system should be used for this purpose. There are several benchmark test systems for studying the LFOs, the most common of which is the two-area test system [82]. This system has also been used in most literature studies. A smart two-area system has been used in this study as a case study. The specifications of this system are shown in Figure 22 and Table III [30].

TABLE III
TEST SYSTEM SPECIFICATIONS

| Item | Description |
|---|---|
| **Generators model** | Sixth-order dynamic model |
| **LPF model** | SGGM |
| **Exciters model** | IEEE type ST1A |
| **PSSs model** | Conventional type STAB1 (Only G2 and G4) |
| **Loads** | Constant power load |
| **LPF operation mode** | Voltage control mode at plant level [47, 48] |
| $T_m$ | 100 ms [94] |

It should be noted that the difference in the generators speeds in the two areas ($\Delta\omega$) is considered as PODC input signal [97, 98]. On the other hand, due to the fact that the transmission of input signals is done through the WAMS [66, 97], so it is necessary to define the constant of time delay, $T_m$, for signal transmission [97].

To evaluate the performance of the proposed PODCs, four scenarios are considered. Although these scenarios are different in terms of disturbance severity, they all lead to LFOs in the power system [30, 32]. These scenarios consider as follows:

- Scenario I: A three-phase fault at bus 8 at $t$ = 1s for 170 ms.
- Scenario II: Outage of line L78-1 at $t$ = 1s for 67 ms.

- Scenario III: Outage of generator G1 at $t$ = 1s for 67 ms.
- Scenario IV: Outage of load L2 at $t$ = 1s for 67 ms.

Also, the robustness of the PODCs is evaluated in terms of the time delay uncertainty of the PODC input signal.

According to the defined scenarios, the simulation results are as follows.

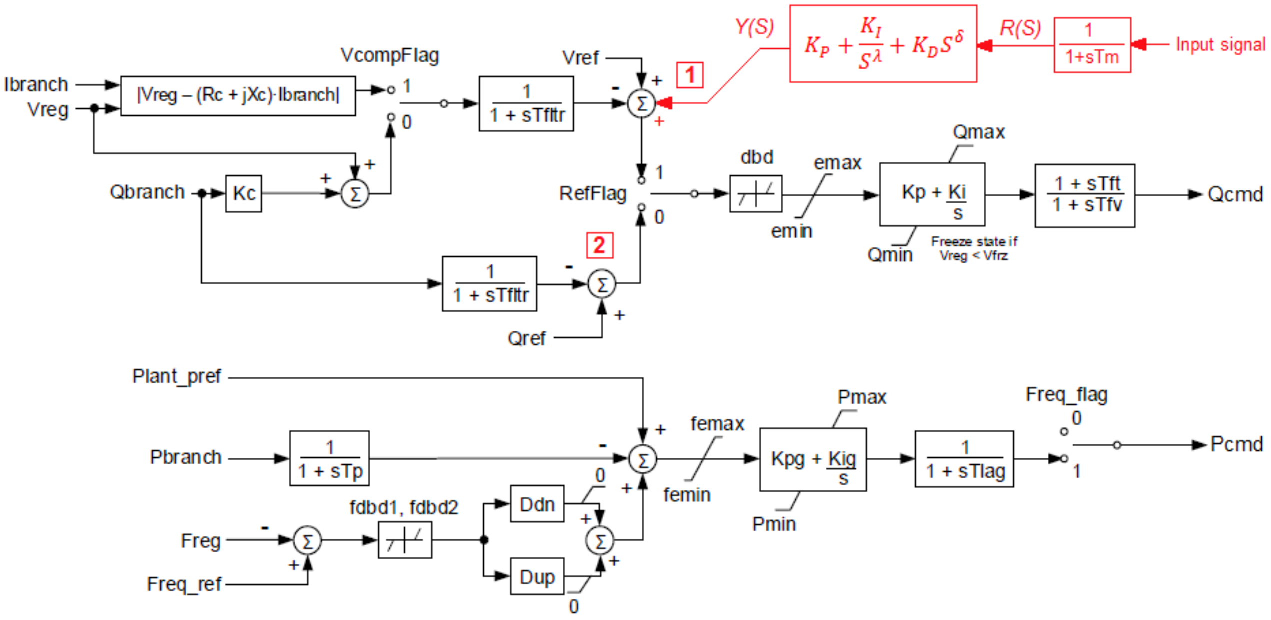

**FIGURE 21.** Structure of REPC_B module with FOPID controlle

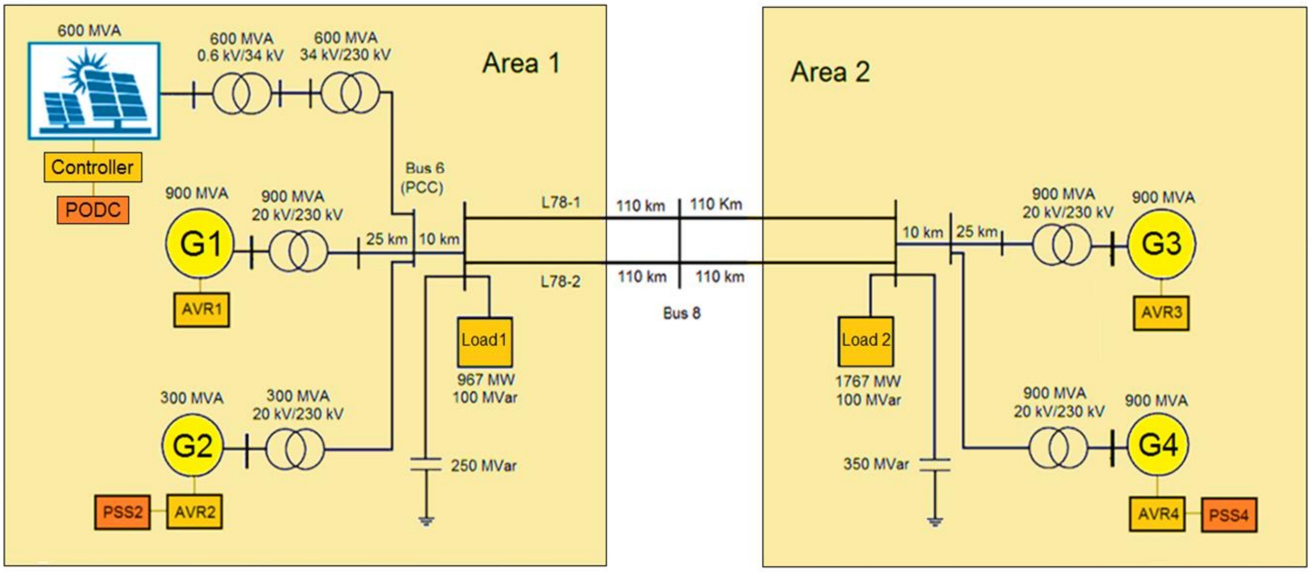

**FIGURE 22.** Schematic structure of two-area test system

This article has been accepted for publication in a future issue of this journal, but has not been fully edited. Content may change prior to final publication. Citation information: DOI 10.1109/ACCESS.2021.3078570, IEEE Access

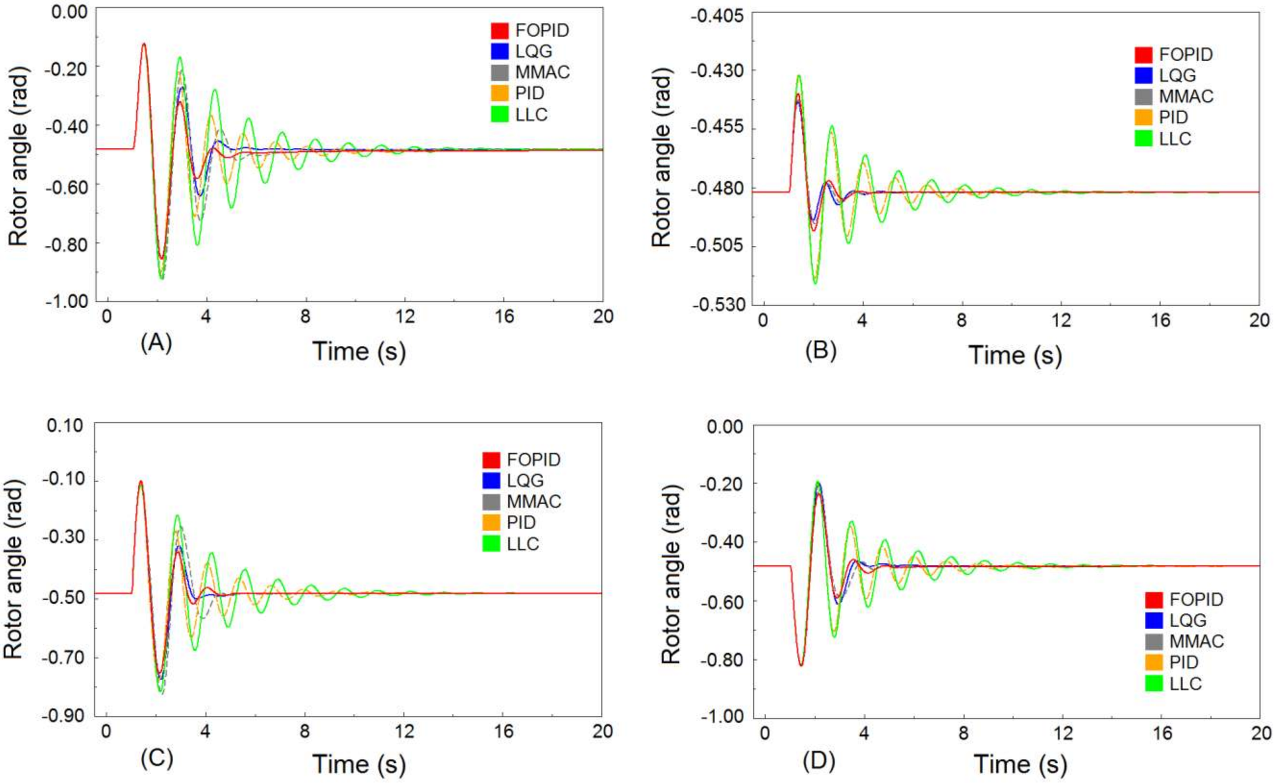

**FIGURE 23.** Rotor angle of generator G1; (A) scenario I, (B) scenario II, (C) scenario III, and (D) scenario IV.

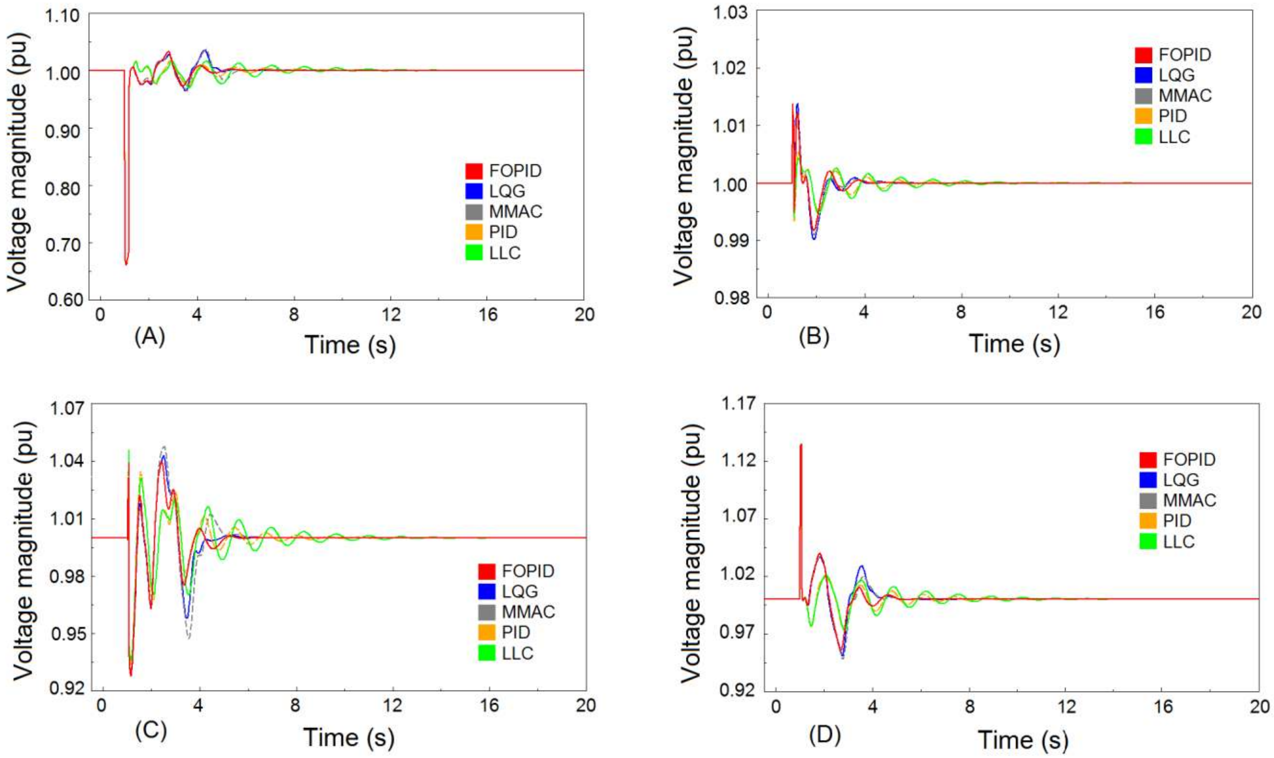

**FIGURE 24.** Voltage magnitude at PCC; (A) scenario I, (B) scenario II, (C) scenario III, and (D) scenario IV.

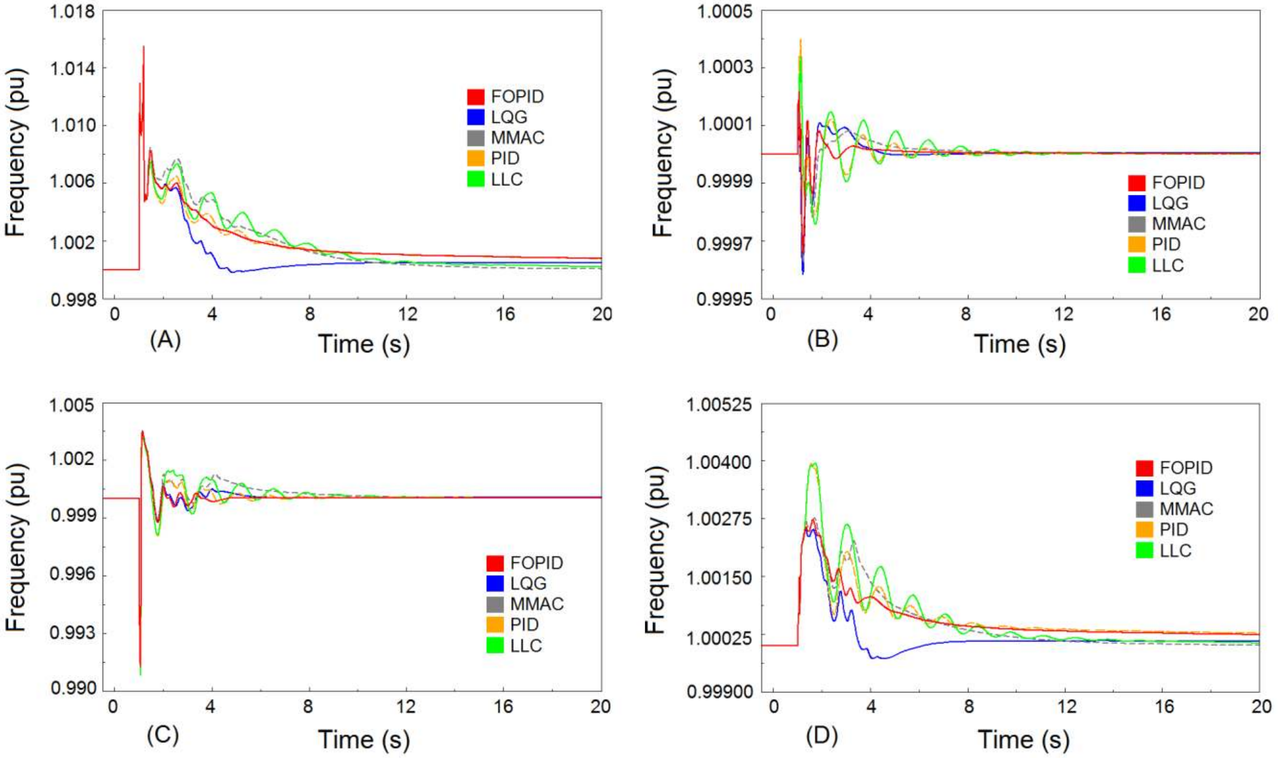

**FIGURE 25.** PCC Frequency; (A) scenario I, (B) scenario II, (C) scenario III, and (D) scenario IV.

As can be seen in Figures 23 to 25, the response of the system to disturbances is different, using different PODCs.

## A. TIME DELAY UNCERTAINTY OF THE PODC INPUT SIGNAL

Time delay uncertainty is one of the major challenges in using the WAMS in smart grids. In these systems, control signals may be received from long distances, so they naturally have a time delay. This time delay can affect the performance of the PODC and cause them to malfunction and cause power system instability. Therefore, controllers must have sufficient robustness against this type of uncertainty in the power systems.

In this section, the robustness of the proposed PODCs in the literature against different time delays is examined.

Accordingly, the performance of the proposed PODCs in scenario I for different time delays is shown in Figure 26. As can be seen from the simulation results, the FOPID controller and the MMAC are robust against time delay uncertainty.

## B. STABILITY AREA OF THE PODCs

One of the indicators needed to compare the performance of PODCs is the range of stability area. In other words, after a large disturbance, a controller with a larger range of stability area causes the system to return to stability more quickly. In this case, a PODC with a smaller range of stability area may cause system instability.

In this section, a comparison is made between the ranges of stability area of the PODCs proposed in the literature. For this purpose, the previous scenarios in a longer period are reviewed as follows:

- Scenario I within 380 ms.
- Scenario III within 145 ms.
- Scenario IV within 320 ms.

The comparison between the proposed PODCs in the literature in terms of the range of stability area is shown in Figures 27 to 29.

As can be seen in the figures, in all scenarios, LLC and PID controllers become unstable quickly and can be said to have small stability areas. It is clear that the FOPID controller shows good stability in all scenarios and has a wide range of stability area. Although the LQG controller is stable in Scenario III, it becomes unstable quickly in the other two scenarios. Regarding MMAC, it can be said that compared to the LQG controller, it has a smaller stability area. This is summarized in Table IV.

TABLE IV
SUMMARY OF THE PERFORMANCE OF THE PROPOSED PODCS

| Control scheme | Damping ratio | Settling time | Stability area | Robustness |
|---|---|---|---|---|
| **LLC** | Low | High | Small | Low |
| **FOPID** | High | Low | large | High |
| **LQG** | High | Low | Medium | Moderate |
| **PID** | Moderate | High | Small | Low |
| **MMAC** | High | Moderate | Small | High |

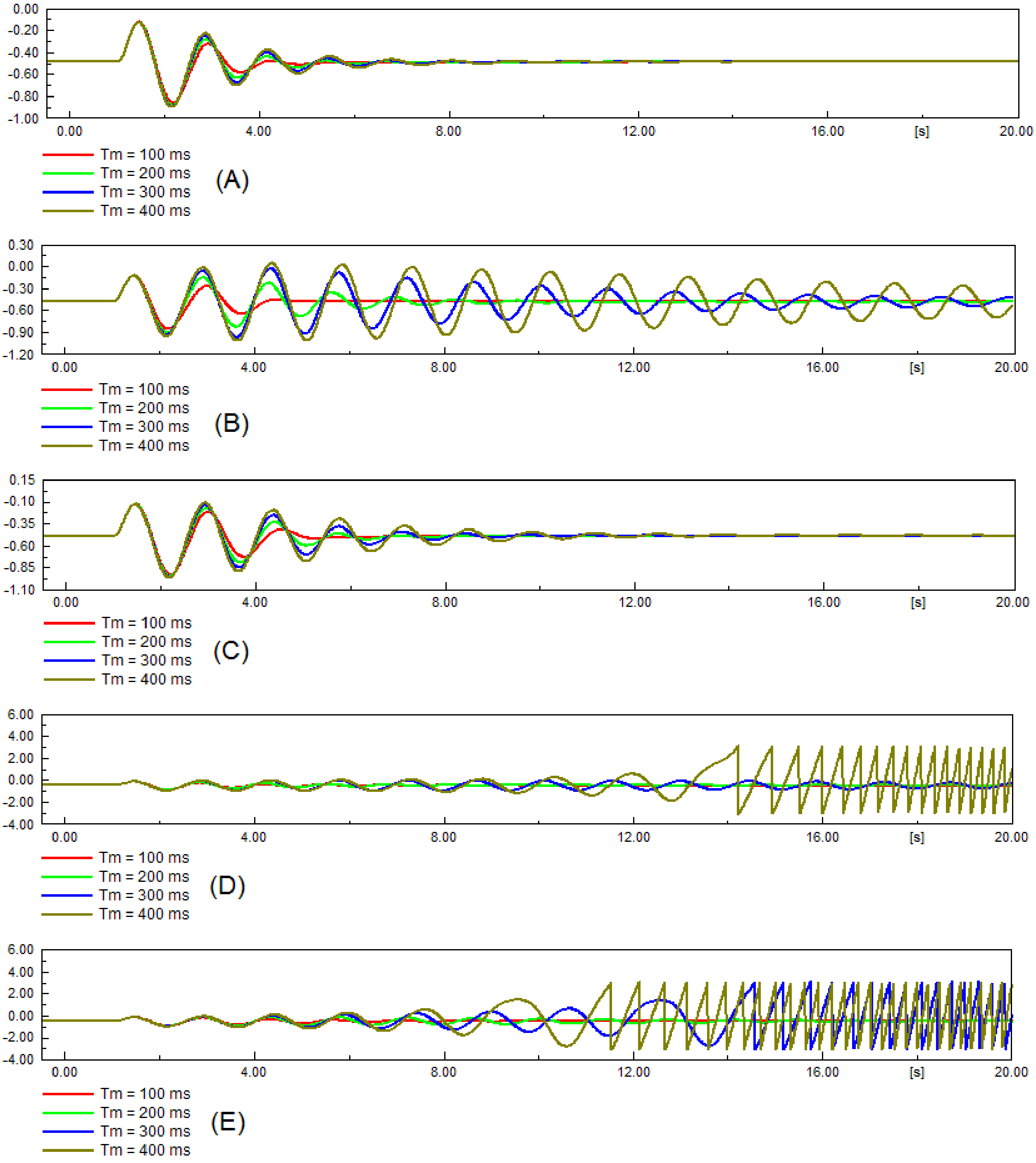

**FIGURE 26.** **Rotor angle of generator G1 for the scenario I for various time delays; (A) FOPID, (B) LQG, (C) MMAC strategy, (D) PID, and (E) LLC.**

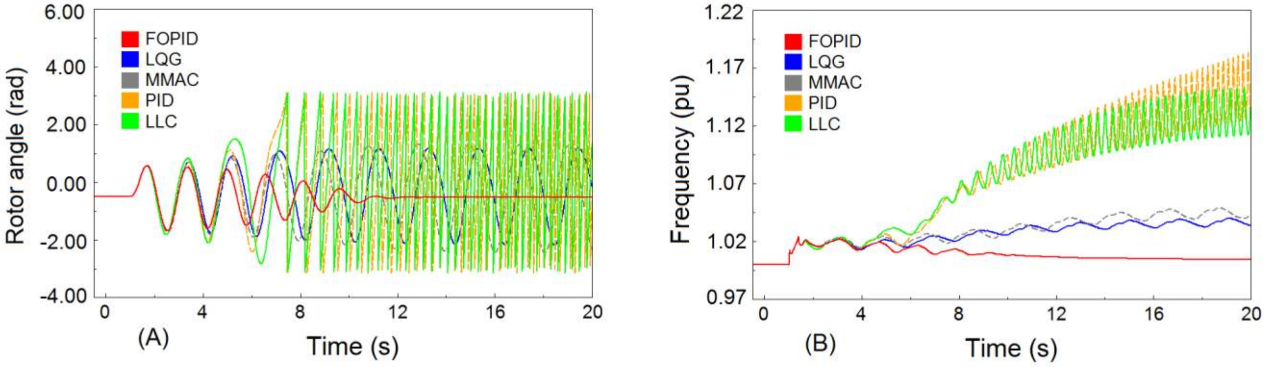

**FIGURE 27.** **Results of scenario I for various PODCs; (A) Rotor angle of generator G1, and (B) PCC frequency.**

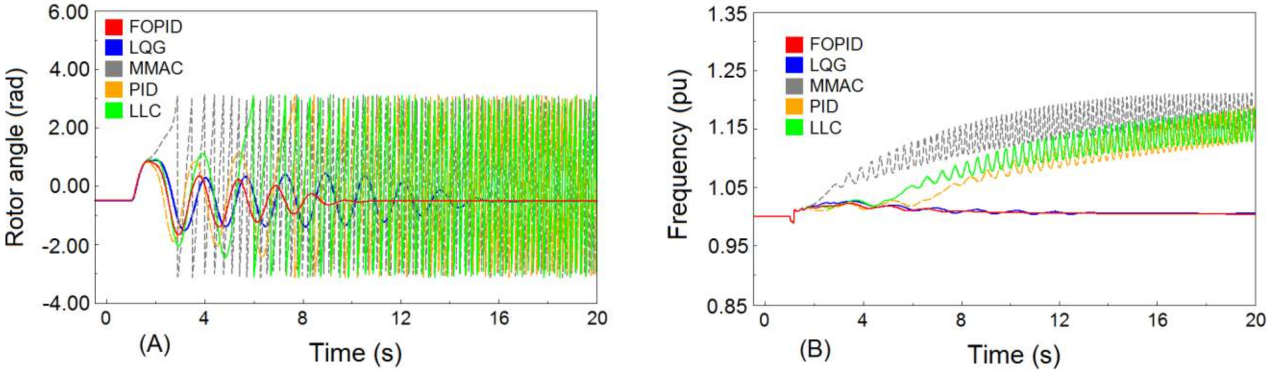

**FIGURE 28.** **Results of scenario III for various PODCs; (A) Rotor angle of generator G1, and (B) PCC frequency.**

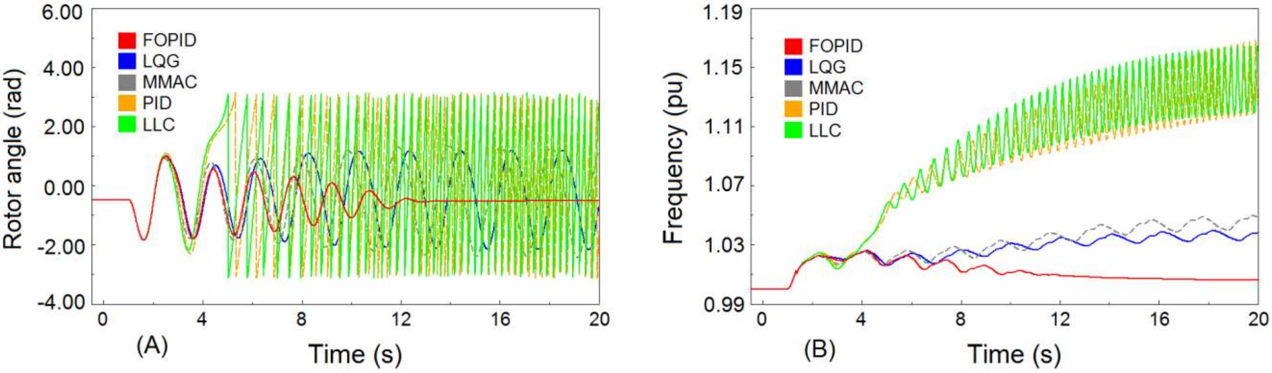

**FIGURE 29.** **Results of scenario IV for various PODCs; (A) Rotor angle of generator G1, and (B) PCC frequency.**

## VII. DISCUSSIONS AND REMARKS

In the studies, several different control methods have been proposed for LFOs damping using LPFs, which are summarized in Table V. Each of the proposed control methods has advantages. In some studies, such as [28], the controllers have been compared and the benefits of each controller have been described. On the other hand, each of the studies has used one of the types of LPF models for simulations, as shown in Table VI. Certainly, with the increasing development of LPFs and the need for a central plant controller, model of this controller is also needed in the LPF model. Therefore, it can be said that with the development of modern power systems and moving towards future power systems, modeling will also lead to the use of the SGGM. The PODC design is generally done using four methods: residue method [20], robust control method [24, 25], optimization-based method [27, 28], and adaptive method [19, 26]. Based on this, the design method of the proposed PODCs in the studies can be summarized in

Table VII. Further studies are needed to compare the performance of different PODCs. For example, the industrialization and commercial aspects of some of these controllers have not yet been identified, but a brief comparison between the various controllers can be made and summarized in Table VIII.

TABLE V
SUMMARY OF THE PROPOSED TYPES OF PODCS IN STUDIES

| Control scheme | References |
|---|---|
| **LLC** | [19-22] |
| **PID Controller** | [23] |
| **LQG Controller** | [24,25] |
| **MMAC Strategy** | [26] |
| **FOPID Controller** | [27, 28] |

TABLE VI
CLASSIFICATION OF LPF MODELING IN THE STUDIES

| References | LPF model |
|---|---|
| **[19, 22, 24, 25, 26]** | FGGM |
| **[20, 21, 23, 27, 28]** | SGGM |

TABLE VII
CLASSIFICATION OF LPF CONTROL STRATEGY

| References | Design method |
|---|---|
| **[21-23, 27, 28]** | Optimization-based method |
| **[19, 26]** | Adaptive method |
| **[24, 25]** | Robust control method |
| **[20]** | Residue-based method |

TABLE VIII
SUMMARY OF PODCS COMPARISON

| Control scheme | Industrialization | Tuning |
|---|---|---|
| **LLC** | Easy | Easy |
| **FOPID** | Difficult | Difficult |
| **LQG** | Moderate | Moderate |
| **PID** | Easy | Easy |
| **MMAC** | Difficult | Difficult |

## VIII. CHALLENGES AND RESEARCH GAPS

Modern power systems are moving toward renewable energy resources to overcome problems related to climate change and global warming. Therefore, REPPs such as LPFs are highly deployed in modern power systems. The high penetration level of LPFs highly reduces the total inertia which affects the stability and security of power systems. So, these types of power plants must be able to increase the power system inertia as well as perform the basic tasks of SGs. For this purpose, they must be able to damp the LFOs by PODCs.

As shown in this paper, different control techniques have been suggested to damp the LFOs by LPFs, but some problems affect the applicability of this issue. On the other hand, it seems that there are still research gaps that need further research. The main challenges and research gaps are as follows:

- **Low capacity of the LPFs:** One of the main challenges is the low capacity of current LPFs. As long as the LPFs do not have high capacity in power systems, they are not effective for LFOs damping. It is important to note that although LPFs based PODCs have acceptable performance, it is necessary to develop the LPFs with capacities above 500 MW in order to be effective for LFOs damping.
- **Uncertainty of power generation of LPFs:** Due to the lack of access to solar radiation at night and also the stochastic behavior of sunlight during the day, power generation stops at night and there is a sharp fluctuation of power production during the day. Therefore, the high intensity of power generation uncertainty has reduced power system reliability. It seems that in this condition, it is practically impossible to depend on this type of power plant for LFOs damping.
- **Auto-tuning:** Given the development of smart grids and taking into account the requirements of modern power systems, one of the most important issues is the auto-tuning of controllers depending on the operation conditions. In fact, the proposed PODCs are now pre-configured and have fixed parameter values for all operating conditions. It seems that in future systems, the tuning of PODCs should be based on online tuning and auto-tuning. This can be a research suggestion for future work.
- **Commercialization and industrialization of PODCs:** one of the important research gaps in this issue is the examination of the capabilities of the proposed modern PODCs such as the FOPID controller for commercialization and industrialization.
- **Low capacity of battery energy storage systems (BESSs) and the impossibility of using virtual SGs (VSGs) [99-102]:** currently, one of the major challenges in power systems is the low capacity of BESSs. Due to the high power of LPFs, this makes it impossible to use VSG and BESS to increase the reliability of LPFs for operation and LFO damping.

Despite the challenges and research gaps mentioned, the possibility of replacing LPF with SGs provides a good opportunity to develop modern power systems in the future.

## IX. CONCLUSION

Due to the growing desire to use renewable energy resources and the high potential of solar energy for electrical power generation, the influence of LPFs in the world is increasing. Accordingly, the LPFs must have the necessary characteristics for power generation in modern power systems. Damping of LFOs is one of the SGs tasks to maintain the power system stability, which is done by

This article has been accepted for publication in a future issue of this journal, but has not been fully edited. Content may change prior to final publication. Citation information: DOI 10.1109/ACCESS.2021.3078570, IEEE Access

PSSs. In recent years, different studies have been conducted to damp the LFOs by REPPs and FACTS devices. This paper is an overview of control methods for LFOs damping by LPFs in power systems. In the studies, various controllers have been proposed as PODC that have been reviewed in this paper. Although the results of the literature review and simulations show the proper performance of the proposed PODCs for LFOs damping by LPFs, there are challenges in this area. It seems that with the advent of modern power systems in the future, this issue is at the beginning and needs further researches. Therefore, it is necessary to study the challenges and provide appropriate solutions to address them in future works.

## APPENDIX

### *REGC_A AND PV1G PARAMETERS, TYPICAL VALUES AND INTERNAL VARIABLES*

| | **Input Parameters** | |
|---|---|---|
| **Name** | **Description** | **Typical Values** |
| **Tfltr** | Terminal voltage filter time constant (s) | 0.01 to 0.02 |
| **Lvpl1** | LVPL gain breakpoint (pu current on mbase / pu voltage) | 1.1 to 1.3 |
| **Zerox** | LVPL zero crossing (pu voltage) | 0.4 |
| **Brkpt** | LVPL breakpoint (pu voltage) | 0.9 |
| **Lvplsw** | low voltage power logic (Enable 1 or disable 0) | - |
| **rrpwr** | Active current up-ramp rate limit on voltage recovery (pu/s) | 10.0 |
| **Tg** | Inverter current regulator lag time constant (s) | 0.02 |
| **Volim** | Voltage limit for high voltage clamp logic (pu) | 1.2 |
| **Iolim** | Current limit for high voltage clamp logic (pu on mbase) | -1.0 to -1.5 |
| **Khv** | High voltage clamp logic acceleration factor | 0.7 |
| **lvpnt0** | Low voltage active current management breakpoint (pu) | 0.4 |
| **lvpnt1** | Low voltage active current management breakpoint (pu) | 0.8 |
| **Iqrmax** | Maximum rate-of-change of reactive current (pu/s) | 999.9 |
| **Iqrmin** | Minimum rate-of-change of reactive current (pu/s) | -999.9 |

| | **Internal Variables** |
|---|---|
| **Name** | **Description** |
| **Vt** | Raw terminal voltage (pu, from network solution) |
| **V** | Filtered terminal voltage (pu) |
| **LVPL** | Active current limit from LVPL logic (pu on mbase) |
| **Iqcmd** | Desired reactive current (pu on mbase) |
| **Ipcmd** | Desired active current (pu on mbase) |
| **Iq** | Actual reactive current (pu on mbase) |

### *REEC_B AND PV1E PARAMETERS, TYPICAL VALUES AND INTERNAL VARIABLES*

| | **Input Parameters** | |
|---|---|---|
| **Name** | **Description** | **Typical Values** |
| **PFflag** | Constant Q (0) or PF (1) local control | - |
| **Vflag** | Local Q (0) or voltage control (1) | - |
| **Qflag** | Bypass (0) or engage (1) inner voltage regulator loop | - |
| **Pqflag** | Priority to reactive current (0) or active current (1) | - |
| **Trv** | Terminal bus voltage filter time constant (s) | 0.01 to 0.02 |
| **Vdip** | Low voltage condition trigger voltage (pu) | 0.0 to 0.9 |
| **Vup** | High voltage condition trigger voltage (pu) | 1.1 to 1.3 |
| **Vref0** | Reference voltage for reactive current injection (pu) | 0.95 to 1.05 |
| **dbd1** | Overvoltage deadband for reactive current injection (pu) | -0.1 to 0.0 |
| **dbd2** | Undervoltage deadband for reactive current injection (pu) | 0.0 to 0.1 |
| **Kqv** | Reactive current injection gain (pu/pu) | 0.0 to 10.0 |
| **Iqhl** | Maximum reactive current injection (pu on mbase) | 1.0 to 1.1 |
| **Iqll** | Minimum reactive current injection (pu on mbase) | -1.1 to -1.0 |
| **Tp** | Active power filter time constant (s) | 0.01 to 0.02 |
| **Qmax** | Maximum reactive power when Vflag = 1 (pu on mbase) | - |
| **Qmin** | Minimum reactive power when Vflag = 1 (pu on mbase) | - |
| **Kqp** | Local Q regulator proportional gain (pu/pu) | - |
| **Kqi** | Local Q regulator integral gain (pu/pu-s) | - |
| **Vmax** | Maximum voltage at inverter terminal bus (pu) | 1.05 to 1.15 |
| **Vmin** | Minimum voltage at inverter terminal bus (pu) | 0.85 to 0.95 |
| **Kvp** | Local voltage regulator proportional gain (pu/pu) | - |
| **Kvi** | Local voltage regulator integral gain (pu/pu-s) | - |
| **Tiq** | Reactive current regulator lag time constant (s) | 0.01 to 0.02 |
| **Tpord** | Inverter power order lag time constant (s) | - |
| **Pmax** | Maximum active power (pu on mbase) | 1.0 |
| **Pmin** | Minimum active power (pu on mbase) | 0.0 |
| **dPmax** | Active power up-ramp limit (pu/s on mbase) | - |
| **dPmin** | Active power down-ramp limit (pu/s on mbase) | - |
| **Imax** | Maximum apparent current (pu on mbase) | 1.0 to 1.3 |

**Internal Variables**

| Name | Description |
|---|---|
| **Vt** | Raw terminal voltage (pu, from network solution) |
| **Vt_filt** | Filtered terminal voltage (pu) |
| **Voltage_dip** | Low/high voltage ride-though condition (Normal=0, VRT=1) |
| **Pe** | Inverter active power (pu on mbase) |
| **Pref** | Inverter active power reference (pu on mbase, from power flow solution or from plant controller model) |
| **Pfaref** | Inverter initial power factor angle (from power flow solution) |
| **Qgen** | Inverter reactive power (pu on mbase) |
| **Qext** | Inverter reactive power reference (pu on mbase, from power flow solution or from plant controller model) |
| **Iqinj** | Supplementary reactive current injection during VRT event (pu on mbase) |
| **Ipmax** | Maximum dynamic active current (pu on mbase) |
| **Ipmin** | Minimum active current (0) |
| **Iqmax** | Maximum dynamic reactive current (pu on mbase) |
| **Iqmin** | Minimum dynamic reactive current (pu on mbase, = -iqmax) |
| **Ipcmd** | Desired active current (pu on mbase) |
| **Iqcmd** | Desired reactive current (pu on mbase) |

## REPC_A PARAMETERS, TYPICAL VALUES AND INTERNAL VARIABLES

**Input Parameters**

| Name | Description | Typical Values |
|---|---|---|
| **RefFlag** | Plant level reactive power (0) or voltage control (1) | - |
| **VcompFlag** | Reactive droop (0) or line drop compensation (1) | - |
| **Freq_flag** | Governor response (disable 0 or enable 1) | 0 |
| **Tfltr** | Voltage and reactive power filter time constant (s) | 0.01 to 0.02 |
| **Vbus** | Monitored bus number | - |
| **FromBus** | Monitored branch "from" bus number | - |
| **ToBus** | Monitored branch "to" bus number | - |
| **Ckt** | Monitored branch circuit designation | - |
| **Rc** | Line drop compensation resistance (pu on mbase) | - |
| **Xc** | Line drop compensation reactance (pu on mbase) when VcompFlag = 1 | - |
| **Kc** | Reactive droop (pu on mbase) when VcompFlag = 0 | - |
| **dbd** | Reactive power deadband (pu on mbase) when<br>RefFlag = 0; Voltage deadband (pu) when RefFlag = 1 | - |
| **emax** | Maximum V/Q error (pu) | - |
| **emin** | Minimum V/Q error (pu) | - |
| **Kp** | V/Q regulator proportional gain (pu/pu)m | - |
| **Kq** | V/Q regulator integral gain (pu/pu-s) | - |
| **Qmax** | Maximum plant reactive power command (pu on mbase) | - |
| **Qmin** | Minimum plant reactive power command (pu on mbase) | - |
| **Vfrz** | Voltage for freezing V/Q regulator integrator (pu) | 0.0 to 0.9 |
| **Tft** | Plant controller Qoutput lead time constant (s) | - |
| **Tfv** | Plant controller Qoutput lag time constant (s) | 0.15 to 5.0 |
| **fdbd1** | Overfrequency deadband for governor response (pu) | 0.01 |
| **fdbd2** | Underfrequency deadband for governor response (pu) | -0.01 |
| **Ddn** | Down regulation droop (pu power/pu freq on mbase) | 20.0 to 33.3 |
| **Dup** | Up regulation droop (pu power/pu freq on mbase) | 0.0 |
| **Tp** | Active power filter time constant (s) | 0.01 to 0.02 |
| **femax** | Maximum power error in droop regulator (pu on mbase) | - |
| **femin** | Minimum power error in droop regulator (pu on mbase) | - |
| **Kpg** | Droop regulator proportional gain (pu/pu) | - |
| **Kig** | Droop regulator integral gain (pu/pu-s) | - |
| **Pmax** | Maximum plant active power command (pu on mbase) | 1.0 |
| **Pmin** | Minimum plant active power command (pu on mbase) | 0.0 |
| **Tlag** | Plant controller Poutput lag time constant (s) | 0.15 to 5.0 |

**Internal Variables**

| Name | Description |
|---|---|
| **Vreg** | Regulated bus voltage (pu, from network solution) |
| **Vref** | Regulated bus initial voltage (pu, from power flow solution) |
| **Ibranch** | Branch current for line drop compensation (pu on mbase) |
| **Qbranch** | Branch reactive power flow for plant Q regulation (pu on mbase) |
| **Qref** | Regulated branch initial reactive power flow (pu, from power flow solution) |
| **Qext** | Reactive power command from plant controller (pu on mbase) |
| **Pbranch** | Branch active power flow for plant P regulation (pu on mbase) |
| **Plant_pref** | Initial branch active power flow (pu on mbase, from power flow solution) |
| **Freq** | Frequency deviation (pu, from network solution) |
| **Freq_ref** | Initial frequency deviation (0) |
| **Pref** | Active power command from plant controller (pu on mbase) |

## ACKNOWLEDGMENT

The work of Hassan Haes Alhelou was supported in part by the Science Foundation Ireland (SFI) through the SFI Strategic Partnership Programme under Grant SFI/15/SPP/E3125, and in part by the University College Dublin (UCD) Energy Institute.

The opinions, findings, and conclusions or recommendations expressed in this material are those of the authors and do not necessarily reflect the views of the Science Foundation Ireland. For the purpose of open access, the author has applied a CC BY public copyright license to any author accepted manuscript version arising from this submission.

## REFERENCES

[1] "Re-thinking 2050: a 100% renewable energy vision for European Union," European Renewable Energy Council; April 2010.

[2] T. Markvart, "*Solar electricity*", New York, NY: John Wiley & Sons; 2000.

[3] Desertec Foundation, [Online]. Available: ⟨http://desertec.org⟩.

[4] H. L. Zhang, J. Baeyens, J. Degrève, G. Cacères, "Concentrated solar power plants: Review and design methodology", *Renewable and sustainable energy reviews*, vol. 22, pp. 466-481, 2013.

[5] "WECC Renewable Energy Modeling Task Force," WECC PV power plant dynamic modeling guide, Western Electricity Coordinating Council, 2014.

[6] IEA, Solar PV power generation in the Sustainable Development Scenario, 2000-2030, IEA, Paris https://www.iea.org/data-and-statistics/charts/solar-pv-power-generation-in-thesustainable-development-scenario-2000-2030.

[7] A. Moghassemi, S. Padmanaban, V. K. Ramachandaramurthy, M. Mitolo, M. Benbouzid M, "A Novel Solar Photovoltaic fed TransZSI-DVR for Power Quality Improvement of Grid-Connected PV Systems," *IEEE Access*, vol. 9, pp. 7263-7279, 2021, 2021.

[8] J. Quintero, V. Vittal, G. T. Heydt, H. Zhang, "The impact of increased penetration of converter control-based generators on power system modes of oscillation", *IEEE Transactions on Power Systems*, vol. 29, no. 5, pp. 2248-2256, 2014.

[9] S. Eftekharnejad, V. Vittal, G. T. Heydt, B. Keel, J. Loehr, "Impact of increased penetration of photovoltaic generation on power systems", *IEEE Transactions on Power Systems*, vol. 28, no. 2, pp. 893-901, 2012.

[10] Y. Zhang, S. Zhu, R. Sparks, I. Green, "Impacts of solar PV generators on power system stability and voltage performance," in *2012 IEEE Power and Energy Society General Meeting*, San Diego, CA, pp. 1-7, 2012.

[11] R. Tonkoski, D. Turcotte, T. H. El-Fouly, "Impact of high PV penetration on voltage profiles in residential neighborhoods", *IEEE Transactions on Sustainable Energy*, vol. 3, no. 3, pp. 518-527, 2012.

[12] S. Eftekharnejad, V. Vittal, G. T. Heydt, B. Keel, J. Loehr, "Small signal stability assessment of power systems with increased penetration of photovoltaic generation: A case study", *IEEE Transactions on Sustainable Energy*, vol. 4, no. 4, pp. 960-967, 2013.

[13] R. Shah, N. Mithulananthan, R. C. Bansal, V. K. Ramachandaramurthy, "A review of key power system stability challenges for large-scale PV integration", *Renewable and Sustainable Energy Reviews*, vol. 41, pp. 1423-1436, 2015.

[14] E. A. Feilat, S. Azzam, A. Al-Salaymeh, "Impact of large PV and wind power plants on voltage and frequency stability of Jordan's national grid", *Sustainable cities and society*, vol. 36, pp. 257-271, 2018.

[15] S. Achilles, S. Schramm, J. Bebic, "Transmission system performance analysis for high penetration photovoltaics", *NREL* (Rep. no. SR-581-42300), 2008.

[16] B. Tamimi, C. Canizares, K. Battacharya, "System stability impact of large-scale and distributed solar photovoltaic generation: the case of Ontario," *IEEE Trans Sustainable Energy*, vol. 4, no. 3, pp. 680-688, 2013.

[17] N. H. Viet, A. Yokoyama, "Impact of fault ride-through characteristics of high-penetration photovoltaic generation on transient stability," in *2010 International Conference on Power System Technology*, Hangzhou, China, pp. 1-7, 2010.

[18] M. Yagami, J. Tamura, "Impact of high-penetration photovoltaic on synchronous generator stability," in *2012 International Conference on Electrical Machines*, Marseille, France, pp. 2092-2097. 2012.

[19] Y. Shen, W. Yao, J. Wen, H. He, "Adaptive wide-area power oscillation damper design for photovoltaic plant considering delay compensation", *IET Generation, Transmission & Distribution*, vol. 11, pp. 4511-4519, 2017.

[20] R. K. Varma, M. Akbari, "Simultaneous fast frequency control and power oscillation damping by utilizing PV solar system as PV-STATCOM", *IEEE Transactions on Sustainable Energy*, vol. 11, no. 1, pp. 415-425, 2019.

[21] M. Saadatmand, B. Mozafari, G. B. Gharehpetian, S. Soleymani, "Optimal Damping Controller Design for Large-scale PV Farms to Damp the Low-frequency Oscillation", *International Journal of Renewable Energy Research (IJRER)*, vol. 9, no. 4, pp. 1672-1680, 2019.

[22] S. Gurung, F. Jurado, S. Naetiladdanon, A. Sangswang, "Optimized tuning of power oscillation damping controllers using probabilistic approach to enhance small-signal stability considering stochastic time delay", *Electrical Engineering*. vol. 101, no. 3, pp. 969-982, 2019.

[23] M. Saadatmand, B. Mozafari, G. B. Gharehpetian, S. Soleymani, "Optimal PID controller of large-scale PV farms for power systems LFO damping", *International Transactions on Electrical Energy Systems*, vol. 30, no. 6, e12372, 2020.

[24] R. Shah, N. Mithulananthan, K. Y. Lee, "Large-scale PV plant with a robust controller considering power oscillation damping", *IEEE Transactions on Energy Conversion*, vol. 28, pp. 106-116, 2012.

[25] R. Shah, N. Mithulananathan, K. Y. Lee, "Design of robust power oscillation damping controller for large-scale PV plant", In *2012 IEEE Power and Energy Society General Meeting*, pp. 1-8, 2012.

[26] L. Zhou, X. Yu, B. Li, C. Zheng, J. Liu, Q. Liu, K. Guo, "Damping Inter-Area Oscillations with Large-Scale PV Plant by Modified Multiple-Model Adaptive Control Strategy", *IEEE Transactions on Sustainable Energy*, vol. 8, pp. 1629-1636, 2017.

[27] M. Saadatmand, B. Mozafari, G. B. Gharehpetian, S. Soleymani, "Optimal fractional-order PID controller of inverter-based power plants for power systems LFO damping", *Turkish Journal of Electrical Engineering & Computer Sciences*, vol. 28, no. 1, pp. 485-499, 2020.

[28] M. Saadatmand, B. Mozafari, G. B. Gharehpetian, S. Soleymani, "Optimal Coordinated Tuning of Power System Stabilizers and Wide-area Measurement-based Fractional-order PID Controller of Large-scale PV Farms for LFO Damping in Smart Grids". *International Transactions on Electrical Energy Systems*, vol.31, no. 2, e12612, 2021.

[29] J. Machowski, Z. Lubosny, J. W. Bialek, and J. R. Bumby, "*Power system dynamics: stability and control*", Hoboken, NJ: John Wiley & Sons, Inc., 2020.

[30] P. Kundur, "*Power system stability and control*", New York: McGraw-Hill, 1994.

[31] M. Klein, G. J. Rogers, P. Kundur, "A fundamental study of inter-area oscillations in power systems," *IEEE Transactions on Power Systems*, vol. 6, no. 3, pp. 914-921, 1991.

[32] B. Pal, B. Chaudhuri, "*Robust control in power systems*", Boston, MA: Springer Science+Business Media, Inc., 2010.

[33] P. Kundur, J. Paserba, V. Ajjarapu, G. Andersson, A. Bose, C. Canizares, N. Hatziargyriou, D. Hill, A. Stankovic, C. Taylor, T. Van Cutsem, "Definition and classification of power system stability IEEE/CIGRE joint task force on stability terms and definitions", *IEEE transactions on Power Systems*, vol. 19, no. 3, pp. 1387-1401, 2004.

[34] N. Hatziargyriou, JV. Milanovic, C. Rahmann, V. Ajjarapu, C. Canizares, I. Erlich, D. Hill, I. Hiskens, I. Kamwa, B. Pal, P. Pourbeik, "Definition and classification of power system stability revisited & extended", *IEEE Transactions on Power Systems*, 2020.

[35] "Stability definitions and characterization of dynamic behavior in systems with high penetration of power electronic interfaced technologies", IEEE Power and Energy Society, Tech. Rep. PESTR77, 2020. https://resourcecenter.ieeepes.org/technical-publications/technicalreports/PES_TP_TR77_PSDP_stability_051320.html

[36] G. Rogers, "*Power system oscillations*", Boston: Kluwer Academic Publishers, 2000.

[37] M. J. Gibbard, DJ Vowles, P Pourbeik, "*Small-signal stability, control and dynamic performance of power systems*", University of Adelaide press; 2015.

[38] D. Mondal, A. Chakrabarti, A. Sengupta, "*Power system small signal stability analysis and control*", Academic Press; 2020 Feb 20.

[39] M. Amin, M. Molinas, "Small-signal stability assessment of power electronics based power systems: A discussion of impedance-and eigenvalue-based methods," *IEEE Transactions on Industry Applications*, vol. 53, no. 5, pp. 5014-5030, 2017.

[40] Y. Wang, X. Wang, Z. Chen, F. Blaabjerg, "Small-signal stability analysis of inverter-fed power systems using component connection method," *IEEE Transactions on Smart Grid*, vol. 9, no. 5, pp. 5301-5010, 2017.

[41] J. Åslund, E. Frisk, "An observer for non-linear differential-algebraic systems," *Automatica*, vol. 42, no. 6, pp. 959-965, 2006.

[42] X. Liu, D. W. C. Ho, "Stabilization of non-linear differential-algebraic equation systems", *International Journal of Control*, vol. 77, no. 7, pp. 671-684, vol.

[43] M. A. Pai, "*Power system stability: analysis by the direct method of Lyapunov*", North-Holland; 1981.

[44] M. Januszewski, J. Machowski, J. W. Bialek, "Application of the direct Lyapunov method to improve damping of power swings by control of UPFC", *IEE Proceedings-Generation, Transmission and Distribution*, vol. 151, no. 2, pp. 252-260, 2004.

[45] R. T. Elliott, A. Ellis, P. Pourbeik, J. J. Sanchez-Gasca, J. Senthil J. Weber, "Generic photovoltaic system models for WECC - A status report," in *2015 IEEE Power & Energy Society General Meeting*, Denver, CO, pp. 1-5, 2015.

[46] A. Ellis, M. Behnke C. Barker, "PV system modeling for grid planning studies," in *2011 37th IEEE Photovoltaic Specialists Conference*, Seattle, WA, pp. 002589-002593, 2011.

[47] "WECC PV plant power flow modeling guide", August 2010.

[48] P. Pourbeik, "Model user guide for generic renewable energy system models", Electric Power Research Institute, 2015.

[49] K. Clark, N. W. Miller, R. Walling, "*Modeling of GE solar photovoltaic plants for grid studies*", General Electric International. Inc, Schenectady, NY. 2010 Apr;12345.

[50] P. Pourbeik *et al*., "Generic Dynamic Models for Modeling Wind Power Plants and Other Renewable Technologies in Large-Scale Power System Studies," *IEEE Transactions on Energy Conversion*, vol. 32, no. 3, pp. 1108-1116, 2017.

[51] "Standard Models for Variable Generation", NERC Special Report, 2010.

[52] O. Wasynczuk, N. A. Anwah, "Modeling and dynamic performance of a self-commutated photovoltaic inverter system," *IEEE Transactions on Energy Conversion*, vol. 4, no. 3, pp. 322-328, 1989.

[53] O. Wasynczuk, "Modeling and dynamic performance of a line-commutated photovoltaic inverter system," *IEEE Transactions on Energy Conversion*, vol. 4, no. 3, pp. 337-343, 1989.

[54] L. Wang, Y. H. Lin, "Dynamic stability analyses of a photovoltaic array connected to a large utility grid," in *2000 IEEE Power Engineering Society Winter Meeting. Conference Proceedings (Cat. No.00CH37077)*, Singapore, vol. 1, pp. 476-480, 2000.

[55] Y.T. Tan, D. Kirschen, N. Jenkins, "A model for PV generation suitable for stability analysis," *IEEE Transactions on Energy Conversion*, vol. 19, no.4, pp.748-755, 2004.

[56] S. Soni, "Solar PV plant model validation for grid integration studies", M.Sc. dissertation, Arizona State University, Tempe, AZ, USA, 2014.

[57] K. Clark, R. A. Walling, N. W. Miller, "Solar photovoltaic (PV) plant models in PSLF," in *2011 IEEE Power and Energy Society General Meeting*, Detroit, MI, USA, pp. 1-5, 2011.

[58] WECC Renewable Energy Modeling Task Force. "Generic Solar Photovoltaic System Dynamic Simulation Model Specification", Salt Lake City: Western Electricity Coordinating Council; 2012.

[59] "EPRI guide on Generic models and model validation for wind and solar PV generation: Technical update," Product ID: 1021763, 2011.

[60] "EPRI guide on Wind and solar PV modeling and model validation: Technical update," Product ID: 1025475, 2012.

[61] WECC Renewable Energy Modeling Task Force. "WECC PV power plant dynamic modeling guide," Western Electricity Coordinating Council, 2014.

[62] E. Muljadi, M. Singh, V. Gevorgian, "User guide for PV dynamic model simulation written on PSCAD platform," No. NREL/TP-5D00-62053. National Renewable Energy Lab (NREL), Golden, CO (United States), 2014.

[63] E. Muljadi, M. Singh, V. Gevorgian, "PSCAD modules representing PV generator," No. NREL/TP-5500-58189. National Renewable Energy Lab (NREL), Golden, CO (United States), 2013.

[64] K. Liao, Z. He, Y. Xu, G. Chen, Z. Y. Dong, K. P. Wong, "A Sliding Mode Based Damping Control of DFIG for Interarea Power Oscillations," *IEEE Transactions on Sustainable Energy*, vol. 8, no. 1, pp. 258-267, 2017.

[65] K. Liao, Y. Xu, Y. Wang, Z. He, H. Marzooghi, "Hybrid fast damping control strategy for doubly fed induction generators against power system inter-area oscillations", *IET Renewable Power Generation*, vol. 12, no. 4, pp. 463-471, 2017.

[66] G. Cai, X. Chen, Z. Sun, D. Yang, C. Liu, H. Li, "A Coordinated Dual-Channel Wide Area Damping Control Strategy for a Doubly-Fed Induction Generator Used for Suppressing Inter-Area Oscillation", *Applied Sciences*, vol. 9, no. 11, 2353, 2019.

[67] P. R. Sahu, P. K. Hota, S. Panda, "Modified whale optimization algorithm for coordinated design of fuzzy lead-lag structure-based SSSC controller and power system stabilizer," *International Transactions on Electrical Energy Systems*, vol. 29, no. 4, e2797, 2019.

[68] A. Nassirharand, H. Karimi, "Closed-form solution for design of lead-lag compensators", *International journal of electrical engineering education*, vol. 41, no. 2, pp. 172-180, 2004.

[69] D. Lee, K. Kim, S. Kim, "Controller Design of an Electric Power Steering System," *IEEE Transactions on Control Systems Technology*, vol. 26, no. 2, pp. 748-755, 2018.

[70] H. Shayeghi, H. A. Shayanfar, A. Safari, R. Aghmasheh, "A robust PSSs design using PSO in a multi-machine environment", *Energy Conversion and Management*, vol. 51, pp. 696-702, 2010.

[71] H. Shabani, B. Vahidi, M. Ebrahimpour, "A robust PID controller based on imperialist competitive algorithm for load-frequency control of power systems", *ISA transactions*, vol. 52, no. 1, pp. 88-95, 2013.

[72] S. Ekinci, B. Hekimoğlu, "Improved kidney-inspired algorithm approach for tuning of PID controller in AVR system", *IEEE Access*, vol. 7, pp. 39935-39947, 2019.

[73] A. Khodabakhshian, R. Hooshmand, "A new PID controller design for automatic generation control of hydro power systems", *International Journal of Electrical Power & Energy Systems*, vol. 32, no. 5, pp. 375-382, 2010.

[74] K. J. Astrom, P. Albertos, J. Quevedo, "PID Control," Automatica *Journal of Control Engineering Practice*, vol. 9, pp.1159-1161, 2001.

[75] K. H. Ang, G. Chong, Y. Li, "PID control system analysis, design, and technology," *IEEE Transactions on Control Systems Technology*, vol. 13, no. 4, pp. 559-576, 2005.

[76] W. K. Ho, K.W. Lim, W. Xu, "Optimal gain phase margin tuning for PID Controllers," *Control Engineering Practice*, vol. 34, no. 8, pp. 1009-1014, 1998.

[77] P. Wang, D. P. Kwok, "Optimal design of PID process controllers based on genetic algorithm," *Control Engineering Practice*, vol. 2, no. 4, pp 641-648, 1994.

[78] V. Mukherjee, S. P. Ghoshal, "Intelligent particle swarm optimized fuzzy PID controller for AVR system," *Electric Power System Research*, vol. 77, no. 12, pp. 1689-1698, 2007.

[79] M. Zamani, M. K. Ghartemani, N. Sadati, M. Parniani, "Design of fractional order PID controller for an AVR using particle swarm optimization," *Control engineering practice*, vol. 17, no. 12, pp. 1380-1387, 2009.

[80] Z. Yachen, H. Yueming, "On PID controllers based on simulated annealing algorithm," in *2008 27th Chinese Control Conference*, Kunming, China, pp. 225-228, 2008.

[81] Z. L. Gaing, "A particle swarm optimization approach for optimum design of PID controller in AVR system," *IEEE Transactions on Energy Conversion*, vol. 19, no. 2, pp. 384-391, 2004.

[82] C. Canizares *et al*., "Benchmark Models for the Analysis and Control of Small-Signal Oscillatory Dynamics in Power Systems," *IEEE Transactions on Power Systems*, vol. 32, no. 1, pp. 715-722, 2017.

[83] K. M. Son, J. K. Park, "On the robust LQG control of TCSC for damping power system oscillations," *IEEE Transactions on Power Systems*, vol. 15, no. 4, pp. 1306-1312, 2000.

[84] A. C. Zolotas, B. Chaudhuri, I. M. Jaimoukha, P. Korba, "A Study on LQG/LTR Control for Damping Inter-Area Oscillations in Power Systems," *IEEE Transactions on Control Systems Technology*, vol. 15, no. 1, pp. 151-160, 2007.

[85] A. M. Yousef, M. Zahran, G. Moustafa, "Improved power system stabilizer by applying LQG controller", In *Advances in Electrical and Computer Engineering Proceeding of 17th international conference on automatic control modeling and simulation*, 2015.

[86] B. Chaudhuri, R. Majumder, B. C. Pal, "Application of multiple-model adaptive control strategy for robust damping of interarea oscillations in power system," *IEEE Transactions on Control Systems Technology*, vol. 12, no. 5, pp. 727-736, 2004.

[87] S. Fekri, M. Athans, A. Pascoal, "Robust multiple model adaptive control (RMMAC): A case study", *International Journal of Adaptive Control and Signal Processing*, vol. 21, no. 1, pp. 1-30, 2007.

[88] K. S. Miller, B. Ross, "*An Introduction to the fractional calculus and fractional differential equations*", New York: John Wiley, 1993.

[89] H. Singh, D. Kumar, D. Baleanu, "*Methods of mathematical modelling: fractional differential equations*," Boca Raton, FL: CRC Press, Taylor & Francis Group, 2020.

[90] K. B. Oldham, J. Spanier, "*The fractional calculus*," New York: Academic Press, 1974.

[91] I. Podlubny, Fractional-order systems and PI/sup /spl lambda//D/sup /spl mu//-controllers," *IEEE Transactions on Automatic Control*, vol. 44, no. 1, pp. 208-214, 1999.

[92] C. A. Monje, Y. Chen, B. M. Vinagre, D. Xue, V. Feliu-Batlle, "*Fractional-order systems and controls: fundamentals and applications*", London: Springer Science & Business Media; 2010.

[93] P. Shah, S. Agashe, "Review of fractional PID controller", *Mechatronics*, vol. 38, pp. 29-41, 2016.

[94] I. Pan, S. Das, "Fractional-order load-frequency control of interconnected power systems using chaotic multi-objective optimization," *Applied Soft Computing*, vol. 29, pp. 328-344, 2015.

[95] L. Chaib, A. Choucha, S. Arif, "Optimal design and tuning of novel fractional order PID power system stabilizer using a new metaheuristic Bat algorithm," *Ain Shams Engineering Journal*, vol. 8, no. 2, pp. 113-125, 2017.

[96] Y. Nie, Y. Zhang, Y. Zhao, B. Fang, L. Zhang, "Wide-area optimal damping control for power systems based on the ITAE criterion," *International Journal of Electrical Power & Energy Systems*, vol. 106, pp. 192-200, 2019.

[97] D. Cai, "Wide area monitoring, protection and control in the future Great Britain power system," Ph.D. dissertation, University of Manchester, Manchester, UK, 2012.

[98] S. K. Kerahroudi, M. M. Alamuti, F. Li, G. A. Taylor, M. E. Bradley, "Application and Requirement of DIgSILENT PowerFactory to MATLAB/Simulink Interface," In: Gonzalez-Longatt FM, Rueda JL (editors). PowerFactory Applications for Power System Analysis. Cham, Switzerland: Springer, pp. 297-322, 2014.

[99] H. Bevrani, T. Ise, Y. Miura, "Virtual synchronous generators: A survey and new perspectives," *International Journal of Electrical Power & Energy Systems*, vol. 54, pp. 244-254, Jan 2014.

[100] Y. Hirase, K. Abe, K. Sugimoto, K. Sakimoto, H. Bevrani, T. Ise, "A novel control approach for virtual synchronous generators to suppress frequency and voltage fluctuations in microgrids," *Applied Energy*, vol. 210, pp. 699-710, Jan 2018.

[101] H. Wu, X. Ruan, D. Yang, X. Chen, W. Zhao, Z. Lv, Q. C. Zhong, "Small-signal modeling and parameters design for virtual synchronous generators," *IEEE Transactions on Industrial Electronics*, vol. 63, no. 7, pp. 4292-4303, Mar 2016.

[102] J. Fang, Y. Tang, H. Li, X. Li, "A battery/ultracapacitor hybrid energy storage system for implementing the power management of virtual synchronous generators," *IEEE Transactions on Power Electronics*. vol. 33, no. 4, pp. 2820-2824, Oct 2017.

**MAHDI SAADATMAND** received the M.Sc. degree in electrical engineering from Amirkabir University of Technology, Tehran, Iran in 2013 and the Ph.D. degree in electrical engineering from Science and Research Branch, Islamic Azad University, Tehran, Iran in 2020. He has authored more than 15 scientific journal and conference papers. His research interests include Power System Dynamics, Smart Grids, Renewable Energy Technologies and Fractional-order control. Since 2019, he has been serving as a reviewer for several high-quality journals.

**GEVORK B. GHAREHPETIAN** (Senior Member, IEEE) received his BS, MS and PhD degrees in electrical engineering in 1987, 1989 and 1996 from Tabriz University, Tabriz, Iran and Amirkabir University of Technology (AUT), Tehran, Iran and Tehran University, Tehran, Iran, respectively, graduating all with First Class Honors. As a PhD student, he has received scholarship from DAAD (German Academic Exchange Service) from 1993 to 1996 and he was with High Voltage Institute of RWTH Aachen, Aachen, Germany. He has been holding the Assistant Professor position at AUT from 1997 to 2003, the position of Associate Professor from 2004 to 2007 and has been Professor since 2007.

He was selected by the MSRT (Ministry of Science Research and Technology) as the distinguished professor of Iran, by IAEEE (Iranian Association of Electrical and Electronics Engineers) as the distinguished researcher of Iran, by Iran Energy Association (IEA) as the best researcher of Iran in the field of energy, by the MSRT as the distinguished researcher of Iran, by the Academy of Science of the Islamic Republic of Iran as the distinguished professor of electrical engineering, by National Elites Foundation as the laureates of Alameh Tabatabaei Award and was awarded the National Prize in 2008, 2010, 2018, 2018, 2019 and 2019, respectively. Based on the Web of Science database (2005-2019), he is among world's top 1% elite scientists according to ESI (Essential Science Indicators) ranking system.

Prof. Gharehpetian is distinguished, senior and distinguished member of CIGRE, IEEE and IAEEE, respectively. Since 2004, he has been the Editor-in-Chief of the Journal of IAEEE. He is the author of more than 1200 journal and conference papers. His teaching and research interests include Smart Grid, Microgrids, FACTS and HVDC Systems, Monitoring of Power Transformers and its Transients.

**ALI MOGHASSEMI** received the B.Sc. and M.Sc. degrees in electrical power engineering from Islamic Azad University, South Tehran Branch, Tehran, Iran, in 2012 and 2015, respectively. He is currently a University Lecturer with the University of Applied Sciences and Technology, Tehran, and also an External Researcher with the Department of Energy Technology, Aalborg University, Esbjerg, Denmark. He has authored or coauthored more than 15 scientific articles in international journals and conferences. He has also published a book and coauthored two book chapters. His current research interests include renewable energy technologies, partial shaded PV, MPPT algorithm, power quality, DVR, voltage disturbances, harmonic, power electronics, Z-source inverter, and Switching Control strategy. Since June 2018, he has been serving as a reviewer for several high-quality journals.

**JOSEP M. GUERRERO** (Fellow, IEEE) earned a Ph.D. degree from the Technical University of Catalonia, Barcelona, Spain, in 2003. He is a full professor with the Department of Energy Technology, Aalborg University, Denmark, where he is the director of the Center for Research on Microgrids. His research interests include distributed energy-storage systems, hierarchical and cooperative control, energy management systems, smart metering, and the Internet of Things for ac/dc microgrid clusters. He was awarded the Institute for Scientific Information "Highly Cited Researcher" by Thomson Reuters for six consecutive years from 2014 to 2019, and he was awarded as a VILLUM Investigator in 2019. He is a Fellow of IEEE and a member of the IEEE Industrial Electronics Society.

**PIERLUIGI SIANO** (M'09-SM'14) received the M.Sc. degree in electronic engineering and the Ph.D. degree in information and electrical engineering from the University of Salerno, Salerno, Italy, in 2001 and 2006, respectively. He is a Professor and Scientific Director of the Smart Grids and Smart Cities Laboratory with the Department of Management & Innovation Systems, University of Salerno. His research activities are centered on demand response, on energy management, on the integration of distributed energy resources in smart grids, on electricity markets and on planning and management of power systems. In these research fields he has co-authored more than 500 articles including more than 300 international journal papers that received in Scopus more than 9450 citations with an H-index equal to 47. He received the award as 2019 Highly cited Researcher by ISI Web of Science Group. He has been the Chair of the IES TC on Smart Grids. He is Editor for the Power & Energy Society Section of IEEE Access, IEEE TRANSACTIONS ON INDUSTRIAL INFORMATICS, IEEE TRANSACTIONS ON INDUSTRIAL ELECTRONICS, Open Journal of the IEEE IES and of IET Renewable Power Generation.

**HASSAN HAES ALHELOU** (Senior Member, IEEE) is with the school of electrical and electronic engineering at University College Dublin, Dublin 4, Ireland. He is also a faculty member at Tishreen University, Lattakia, Syria. He is included in the 2018 and 2019 Publons list of the top 1% best reviewer and researchers in the field of engineering. He was the recipient of the Outstanding Reviewer Award from Energy Conversion and Management Journal in 2016, ISA Transactions Journal in 2018, Applied Energy Journal in 2019, and many other Awards. He was the recipient of the best young researcher in the Arab Student Forum Creative among 61 researchers from 16 countries at Alexandria University, Egypt, 2011. He has published more than 130 research papers in the high quality peer-reviewed journals and international conferences. He has also performed reviews for high prestigious journals including IEEE Transactions on Industrial Informatics, IEEE Transactions on Industrial Electronics, Energy Conversion and Management, Applied Energy, International Journal of Electrical Power & Energy Systems. He has participated in more than 15 industrial projects. His major research interests are Power systems, Power system dynamics, Power system operation and control, Dynamic state estimation, Frequency control, Smart grids, Micro-grids, Demand response, Load shedding, and Power system protection.